

# A fast second-order implicit difference method for time-space fractional advection-diffusion equation

Yong-Liang Zhao<sup>a</sup> \*; Ting-Zhu Huang<sup>a</sup> †; Xian-Ming Gu<sup>a</sup> ‡; Wei-Hua Luo<sup>b</sup> §

*a. School of Mathematical Sciences,*

*University of Electronic Science and Technology of China,  
Chengdu, Sichuan 611731, P.R. China*

*b. Data Recovery Key Laboratory of Sichuan Province,  
Neijiang Normal University, Neijiang, Sichuan, 641100, P.R. China*

## Abstract

In this paper, we consider a fast and second-order implicit difference method for approximation of a class of time-space fractional variable coefficients advection-diffusion equation. To begin with, we construct an implicit difference scheme, based on  $L2 - 1_\sigma$  formula [A. Alikhanov, A new difference scheme for the time fractional diffusion equation, *J. Comput. Phys.*, 280 (2015)] for the temporal discretization and weighted and shifted Grünwald method for the spatial discretization. Then, unconditional stability of the implicit difference scheme is proved, and we theoretically and numerically show that it converges in the  $L_2$ -norm with the optimal order  $\mathcal{O}(\tau^2 + h^2)$  with time step  $\tau$  and mesh size  $h$ . Secondly, three fast Krylov subspace solvers with suitable circulant preconditioners are designed to solve the discretized linear systems with the Toeplitz matrix. In each iterative step, these methods reduce the memory requirement of the resulting linear equations from  $\mathcal{O}(N^2)$  to  $\mathcal{O}(N)$  and the computational complexity from  $\mathcal{O}(N^3)$  to  $\mathcal{O}(N \log N)$ , where  $N$  is the number of grid nodes. Finally, numerical experiments are carried out to demonstrate that these methods are more practical than the traditional direct solvers of the implicit difference methods, in terms of memory requirement and computational cost.

**Key words:** Fractional advection-diffusion equation; Weighted and shifted Grünwald scheme;  $L2 - 1_\sigma$  formula; Krylov subspace method; Toeplitz matrix; Fast Fourier transform; Circulant preconditioner.

**AMS Classification:** 65F12; 65L05; 65N22.

## 1 Introduction

This article is concerned with a fast second-order implicit difference method (IDM) for solving the initial-boundary value problem of the time-space fractional advection-diffusion equation

---

\**E-mail address:* uestc\_ylzhao@sina.com

†*Corresponding author. E-mail address:* tingzhuhuang@126.com. Tel: +86 28 61831608, fax: +86 28 61831280.

‡*E-mail address:* guxianming@live.cn, x.m.gu@rug.nl

§*E-mail address:* huaweiluo2012@163.com

(TSFADE) [1, 2]:

$$\begin{cases} D_{0,t}^\theta u(x,t) = -d_+(t)D_{0,x}^\alpha u(x,t) - d_-(t)D_{x,L}^\alpha u(x,t) \\ \quad + e_+(t)D_{0,x}^\beta u(x,t) + e_-(t)D_{x,L}^\beta u(x,t) + f(x,t), \\ u(x,0) = u_0(x), \quad 0 \leq x \leq L, \\ u(0,t) = u(L,t) = 0, \quad 0 \leq t \leq T, \end{cases} \quad (1.1)$$

where  $\theta, \alpha \in (0, 1]$ ,  $\beta \in (1, 2]$ ,  $0 < x < L$ , and  $0 < t \leq T$ . Here, the parameters  $\theta, \alpha$  and  $\beta$  are the order of the TSFADE,  $f(x, t)$  is the source term, and diffusion coefficient functions  $d_\pm(t)$  and  $e_\pm(t)$  are non-negative under the assumption that the flow is from left to right. The TSFADE (1.1) can be regarded as generalizations of classical advection-diffusion equations with the first-order time derivative replaced by the Caputo fractional derivative of order  $\theta \in (0, 1]$ , and the first-order and second-order space derivatives replaced by the two-sided Riemann-Liouville fractional derivatives of order  $\alpha \in (0, 1]$  and  $\beta \in (1, 2]$ . Namely, the time fractional derivative in (1.1) is the Caputo fractional derivative [3, 4] of order  $\theta$  denoted by

$$D_{0,t}^\theta u(x,t) = \frac{1}{\Gamma(1-\theta)} \int_0^t \frac{\partial u(x,\xi)}{\partial \xi} \frac{d\xi}{(t-\xi)^\theta}, \quad (1.2)$$

and the left ( $D_{0,x}^\alpha, D_{0,x}^\beta$ ) and right ( $D_{x,L}^\alpha, D_{x,L}^\beta$ ) space fractional derivatives in (1.1) are the Riemann-Liouville fractional derivatives [3, 4] which can be defined by

(1) left Riemann-Liouville fractional derivative:

$$D_{0,x}^\gamma u(x,t) = \frac{1}{\Gamma(n-\gamma)} \frac{d^n}{dx^n} \int_0^x \frac{u(\eta,t)}{(x-\eta)^{\gamma-n+1}} d\eta, \quad (1.3)$$

(2) right Riemann-Liouville fractional derivative:

$$D_{x,L}^\gamma u(x,t) = \frac{(-1)^n}{\Gamma(n-\gamma)} \frac{d^n}{dx^n} \int_x^L \frac{u(\eta,t)}{(\eta-x)^{\gamma-n+1}} d\eta, \quad (1.4)$$

where  $\Gamma(\cdot)$  denotes the Gamma function and  $n-1 \leq \gamma < n$  ( $n$  is a positive integer). In reality, when  $\theta = \alpha = 1$  and  $\beta = 2$ , the above equation reduces to the classical advection-diffusion equation (ADE).

There have been many study and application of the fractional ADE. It should be point out that the fractional ADE provides more adequate and accurate description of the movement of solute in an aquifer than traditional second-order ADEs do [5, 6], and also used to approach the description of transport dynamics in complex systems which are governed by anomalous diffusion and non-exponential relaxation patterns [7]. Moreover, the fractional ADE is a more suitable model for many problems, such as engineering, physics, chemistry, entropy [8] and hydrology [9]. To obtain the analytical solutions of fractional partial differential equations [3], numerous analytical methods, such as the Fourier transform method, Adomians decomposition method [10], the Laplace transform method [11], shifted Legendre polynomials [12], and the Mellin transform method, have been developed. Since there are very few cases in which the closed-form analytical solutions are available, or the obtained analytical solutions are less practical (expressed by the transcendental functions or infinite series). Researches on numerical approximation and techniques for the solution of fractional difference equations (FDEs) have attracted intensive interest; see [13–21] and references therein.

Regarding numerical methods for fractional advection-diffusion problems. In the last years, most early established numerical methods are developed for handling the space fractional ADE or the time fractional ADE. For the time fractional ADE, many early implicit numerical methods are derived by the combination of the  $L1$  approximate formula [22, 23]. These methods are unconditionally stable, but the time accuracy can not meet second order. In addition, some other related numerical methods have already been proposed for handling the time fractional ADE; see e.g. [27–30] for details. On the other hand, for the space fractional ADE, many researchers exploited the conventional shifted Grünwald discretization [24] and the implicit Euler (or Crank-Nicolson) time-step discretization for two-sided Riemann-Liouville fractional derivatives and the first order time derivative, respectively. Later, Sousa and Li [25] derived a weighted finite difference scheme for producing the novel numerical methods, which achieved the second order accuracy in both time and space for space fractional ADE. Qu and Lei et al. employed circulant and skew-circulant splitting iteration, which can reduce the required algorithm storage, for implementing the above mentioned second order numerical method; see [26] for details.

Contrarily, although the numerical methods for space (or time) fractional ADE are extensively investigated in the past researches, the work about numerically handling the TSFADE is not too much. Firstly, Liu et al. [24], Zhang [31, 32], Shao & Ma [33], and Qin & Zhang [34] have worked out a series of studies about constructing the implicit difference scheme (IDS) for TSFADE, however all these numerical scheme can achieve the convergence with first order accuracy in both space and time from both the theoretical and numerical perspectives. Liu et al. [1] also considered a space-time fractional advection dispersion equation and the implicit difference method proposed by them has convergence  $\mathcal{O}(\tau+h)$ . Then, Shen et al. [35] presented an explicit difference approximation with convergence  $\mathcal{O}(\tau+h)$  and an implicit difference approximation with convergence rate  $\mathcal{O}(\tau^{2-\alpha}+h)$ . Inspired by Liu’s paper [1], Zhao et al. [2] introduced preconditioned iterative methods to reduce the amount of computation while solving TSFADE, but its convergence can only reach  $\mathcal{O}(\tau^{2-\alpha}+h)$ . Later, Gu et al. [58] established fast solution techniques to solve the discretization linear system of the time-space fractional convection-diffusion equation, which has convergence rate  $\mathcal{O}(\tau^2+h^2)$ . Furthermore, most of these methods have no complete theoretical analysis for both stability and convergence, refer to [36–39] for details.

Since the fractional differential operator is nonlocal, it was shown that a naive discretization of the FDE, even though implicit, leads to unconditionally unstable [16, 17]. Moreover, traditional methods for solving FDEs tend to generate full coefficient matrices, which require computational cost of  $\mathcal{O}(N^3)$  and storage of  $\mathcal{O}(N^2)$  [40, 41]. There is no doubt that if  $N$  is not small, both time consuming and storage capacity are tremendous, and this situation is what we try to avoid. To optimize the computational complexity, Meerschaet and Tadjeran [16, 17] proposed a shifted Grünwald discretization to approximate FDEs, which has been proved to be unconditionally stable. Later, Wang, Wang and Sircar [42] discovered that the full coefficient matrix by the shifted Grünwald scheme holds a Toeplitz-like structure. More precisely, this matrix can be written as a sum of diagonal-multiply-Toeplitz matrices. This means that the matrix-vector multiplication for Toeplitz matrix can be computed by the fast Fourier transform (FFT) with  $\mathcal{O}(N \log N)$  operations [43], and the storage requirement is reduced to  $\mathcal{O}(N)$ . Thanks to the Toeplitz-like structure, Wang and Wang [44] employed the CGNR method to solve discretized linear system of FDE by the Meerschaet-Tadjeran’s method, and the cost of each iteration is  $\mathcal{O}(N \log N)$ . Numerical experiments indicate that the CGNR method is fast when the diffusion coefficients are small enough, namely, the discretized system is well-conditioned. Nevertheless, the discretized system will become ill-conditioned when the diffusion coefficients are not small,

hence the CGNR method converges very slowly. To overcome this shortcoming, Zhao et al. have extended the precondition technique, for handling the Toeplitz-like matrix with structure as the sum of diagonal-multiply-Toeplitz matrices [2]. Their results related to the promising acceleration of the convergence of the iterative methods, while solving (1.1), see [45–47] for other preconditioning methods. For the same reason, we propose three preconditioned iterative methods, i.e., the preconditioned biconjugate gradient stabilized (BiCGSTAB) method [48], the preconditioned biconjugate residual stabilized (BiCRSTAB) method and the preconditioned generalized product-type solvers based on BiCOR (GPBiCOR( $m, \ell$ )) method [49], and observe results related to the acceleration of the convergence of the iterative methods, while solving (1.1).

The rest of this paper is arranged as follows. In Section 2, the implicit difference scheme for (1.1) is presented, and we prove that this scheme is unconditionally stable and convergent with the accuracy of  $\mathcal{O}(\tau^2 + h^2)$ . In Section 3, the BiCGSTAB method, the BiCRSTAB method and the GPBiCOR( $m, \ell$ ) method with suitable circulant preconditioners are proposed to solve the discretized linear system. In Section 4, numerical results are reported to demonstrate the efficiency of our numerical approaches, and concluding remarks are given in Section 5.

## 2 An implicit difference scheme for TSFADE

In this section, we present an implicit difference method for discretizing the TSFADE defined by (1.1). Unlike the former numerical approaches [1, 2, 35], we exploit henceforth two-sided fractional derivatives to approximate the Riemann-Liouville derivatives in (1.3) and (1.4). we can show that, by two-sided fractional derivatives, this proposed method is also unconditionally stable and convergent second order accuracy in both time and space.

### 2.1 Discretization of the TSFADE

In order to derive the proposed scheme, we first introduce the mesh  $\bar{\omega}_{h\tau} = \bar{\omega}_h \times \bar{\omega}_\tau$ , where  $\bar{\omega}_h = \{x_i = ih, i = 0, 1, \dots, N; x_0 = 0, x_N = L\}$  and  $\bar{\omega}_\tau = \{t_j = j\tau, j = 0, 1, \dots, M; t_M = T\}$ . Besides,  $\mathbf{v} = \{v_i \mid 0 \leq i \leq N\}$  be any grid function. Then the following lemma introduced in [50] gives a description on the Caputo fractional derivative discretization.

**Lemma 2.1.** *suppose  $0 < \theta < 1$ ,  $\sigma = 1 - \frac{\theta}{2}$ ,  $y(t) \in \mathcal{C}^3[0, T]$ , and  $t_{j+\sigma} = (j + \sigma)\tau$ . Then*

$$\left| D_{0,t}^\theta y(t) - \Delta_{0,t_{j+\sigma}}^\theta y(t) \right| = \mathcal{O}(\tau^{3-\theta}),$$

where

$$\Delta_{0,t_{j+\sigma}}^\theta y(t) = \frac{\tau^{-\theta}}{\Gamma(2-\theta)} \sum_{s=0}^j c_{j-s}^{(\theta,\sigma)} [y(t_{s+1}) - y(t_s)], \quad (2.1)$$

and for  $j = 0$ ,  $c_0^{(\theta,\sigma)} = a_0^{(\theta,\sigma)}$ , for  $j \geq 1$ ,

$$c_s^{(\theta,\sigma)} = \begin{cases} a_0^{(\theta,\sigma)} + b_1^{(\theta,\sigma)}, & s = 0, \\ a_s^{(\theta,\sigma)} + b_{s+1}^{(\theta,\sigma)} - b_s^{(\theta,\sigma)}, & 1 \leq s \leq j-1, \\ a_j^{(\theta,\sigma)} - b_j^{(\theta,\sigma)}, & s = j, \end{cases}$$

in which  $a_0^{(\theta,\sigma)} = \sigma^{1-\theta}$ ,  $a_l^{(\theta,\sigma)} = (l + \sigma)^{1-\theta} - (l - 1 + \sigma)^{1-\theta}$ , for  $l \geq 1$ ; and  $b_l^{(\theta,\sigma)} = \frac{1}{2-\theta} \left[ (l + \sigma)^{2-\theta} - (l - 1 + \sigma)^{2-\theta} \right] - \frac{1}{2} \left[ (l + \sigma)^{1-\theta} - (l - 1 + \sigma)^{1-\theta} \right]$ .

On the other hand, the Riemann-Liouville derivatives (1.3) and (1.4) can be approximated by the weighted and shifted Grünwald difference (WSGD) operator in Deng's paper [51] (in this paper  $(p, q) = (1, 0)$ ), for parameter  $\gamma$ , i.e.,

$$D_{0,x}^\gamma u(x, t) = \frac{1}{h^\gamma} \sum_{k=0}^{\lceil \frac{x}{h} \rceil + 1} \omega_k^{(\gamma)} u(x - (k-1)h, t) + \mathcal{O}(h^2), \quad (2.2)$$

$$D_{x,L}^\gamma u(x, t) = \frac{1}{h^\gamma} \sum_{k=0}^{\lceil \frac{L-x}{h} \rceil + 1} \omega_k^{(\gamma)} u(x + (k-1)h, t) + \mathcal{O}(h^2). \quad (2.3)$$

Let  $u_i^j$  represent the numerical approximation of  $u(x_i, t_j)$ , then we denote that

$$\delta_{x,+}^\gamma u_i^j = \frac{1}{h^\gamma} \sum_{k=0}^{i+1} \omega_k^{(\gamma)} u_{i-k+1}^j, \quad \delta_{x,-}^\gamma u_i^j = \frac{1}{h^\gamma} \sum_{k=0}^{N-i+1} \omega_k^{(\gamma)} u_{i+k-1}^j,$$

where

$$\omega_0^{(\gamma)} = \frac{\gamma}{2} g_0^{(\gamma)}, \quad \omega_k^{(\gamma)} = \frac{\gamma}{2} g_k^{(\gamma)} + \frac{2-\gamma}{2} g_{k-1}^{(\gamma)}, \quad k \geq 1,$$

and

$$g_0^{(\gamma)} = 1, \quad g_k^{(\gamma)} = \left( 1 - \frac{\gamma+1}{k} \right) g_{k-1}^{(\gamma)}, \quad k = 1, 2, \dots$$

Suppose  $u(x, t) \in \mathcal{C}_{x,t}^{4,3}[0, L] \times [0, T]$  is a solution of the TSADE (1.1). For simplicity, we introduce some symbols

$$u_i^{(\sigma)} = \sigma u_i^{j+1} + (1 - \sigma) u_i^j, \quad d_\pm^{j+\sigma} = d_\pm(t_{j+\sigma}), \quad e_\pm^{j+\sigma} = e_\pm(t_{j+\sigma}), \quad f_i^{j+\sigma} = f(x_i, t_{j+\sigma}),$$

$$\delta_h^{\alpha,\beta} u_i^{(\sigma)} = -d_+^{j+\sigma} \delta_{x,+}^\alpha u_i^{(\sigma)} - d_-^{j+\sigma} \delta_{x,-}^\alpha u_i^{(\sigma)} + e_+^{j+\sigma} \delta_{x,+}^\beta u_i^{(\sigma)} + e_-^{j+\sigma} \delta_{x,-}^\beta u_i^{(\sigma)}.$$

Using (2.1)-(2.3), we shall see that the solution of (1.1) can be approximated by the following implicit difference scheme for  $(x, t) = (x_i, t_{j+\sigma}) \in \bar{\omega}_{h\tau}$ ,  $i = 1, 2, \dots, N-1$ ,  $j = 0, 1, \dots, M-1$ :

$$\Delta_{0,t_{j+\sigma}}^\theta u_i = \delta_h^{\alpha,\beta} u_i^{(\sigma)} + f_i^{j+\sigma}.$$

Then we derive the implicit difference schemes with the approximation order  $\mathcal{O}(\tau^2 + h^2)$ :

$$\begin{cases} \Delta_{0,t_{j+\sigma}}^\theta u_i = \delta_h^{\alpha,\beta} u_i^{(\sigma)} + f_i^{j+\sigma}, & 1 \leq i \leq N-1, \quad 0 \leq j \leq M-1, \\ u_i^0 = u_0(x_i), & 1 \leq i \leq N-1, \\ u_0^j = u_N^j = 0, & 0 \leq j \leq M-1. \end{cases} \quad (2.4)$$

It is interesting to note that for  $\theta \rightarrow 1$ , we obtain the Crank-Nicolson difference scheme.

## 2.2 Analysis of the implicit difference scheme

In this subsection, we analyze the stability and convergence for the implicit difference scheme (2.4). Before proving the stability and convergence of the implicit difference scheme (2.4), we provide some properties of the coefficients  $\omega_k^{(\alpha)}$  and  $\omega_k^{(\beta)}$ , which are derived from  $g_k^{(\alpha)}$  and  $g_k^{(\beta)}$ , respectively.

**Lemma 2.2.** [1, 2, 52] Suppose that  $0 < \alpha < 1$ , then the coefficients  $g_k^{(\alpha)}$  satisfy

$$\begin{cases} g_0^{(\alpha)} = 1, & g_1^{(\alpha)} = -\alpha < 0, & g_k^{(\alpha)} = \mathcal{O}(k^{-(\alpha+1)}), & k = 1, 2, \dots, \\ g_1^{(\alpha)} < g_2^{(\alpha)} < g_3^{(\alpha)} < \dots < 0, \\ \sum_{k=0}^{\infty} g_k^{(\alpha)} = 0, & \sum_{k=0}^N g_k^{(\alpha)} > 0, & N \geq 1. \end{cases}$$

**Lemma 2.3.** [1, 2, 52] Suppose that  $1 < \beta \leq 2$ , then the coefficients  $g_k^{(\beta)}$  satisfy

$$\begin{cases} g_0^{(\beta)} = 1, & g_1^{(\beta)} = -\beta < 0, & g_k^{(\beta)} = \mathcal{O}(k^{-(\beta+1)}), & k = 1, 2, \dots, \\ 1 \geq g_2^{(\beta)} \geq g_3^{(\beta)} \geq \dots \geq 0, \\ \sum_{k=0}^{\infty} g_k^{(\beta)} = 0, & \sum_{k=0}^N g_k^{(\beta)} < 0, & N \geq 2. \end{cases}$$

We obtain the following two lemmas immediately, since the properties of  $\omega_k^{(\alpha)}$  and  $\omega_k^{(\beta)}$  are similar to  $g_k^{(\alpha)}$  and  $g_k^{(\beta)}$ , respectively. From Lemma 2.2, the properties of the coefficients  $\omega_k^{(\alpha)}$  are given as follows.

**Lemma 2.4.** [52] Suppose that  $0 < \alpha < 1$ , then the coefficients  $\omega_k^{(\alpha)}$  satisfy

$$\begin{cases} \omega_0^{(\alpha)} = \frac{\alpha}{2} > 0, & \omega_1^{(\alpha)} = \frac{2-\alpha-\alpha^2}{2} > 0, & \omega_2^{(\alpha)} = \frac{\alpha(\alpha^2+\alpha-4)}{4} < 0, \\ \omega_2^{(\alpha)} < \omega_3^{(\alpha)} < \omega_4^{(\alpha)} < \dots < 0, & \omega_0^{(\alpha)} + \omega_2^{(\alpha)} < 0, \\ \sum_{k=0}^{\infty} \omega_k^{(\alpha)} = 0, & \sum_{k=0}^N \omega_k^{(\alpha)} > 0, & N \geq 1. \end{cases}$$

In the same way, the properties of coefficients  $\omega_k^{(\beta)}$  are expressed in next lemma.

**Lemma 2.5.** [52] Suppose that  $1 < \beta < 2$ , then the coefficients  $\omega_k^{(\beta)}$  satisfy

$$\begin{cases} \omega_0^{(\beta)} = \frac{\beta}{2} > 0, & \omega_1^{(\beta)} = \frac{2-\beta-\beta^2}{2} < 0, & \omega_2^{(\beta)} = \frac{\beta(\beta^2+\beta-4)}{4}, \\ 1 \geq \omega_0^{(\beta)} \geq \omega_3^{(\beta)} \geq \omega_4^{(\beta)} \geq \dots \geq 0, & \omega_0^{(\beta)} + \omega_2^{(\beta)} > 0, \\ \sum_{k=0}^{\infty} \omega_k^{(\beta)} = 0, & \sum_{k=0}^N \omega_k^{(\beta)} < 0, & N \geq 2. \end{cases}$$

In the rest of this paper, we define the discrete inner product and the corresponding discrete  $L_2$ -norm as follows,

$$(\mathbf{u}, \mathbf{v}) = h \sum_{i=1}^{N-1} u_i v_i, \quad \|\mathbf{u}\| = \sqrt{(\mathbf{u}, \mathbf{u})}, \quad \text{for } \forall \mathbf{u}, \mathbf{v} \in V_h,$$

where

$$V_h = \{\mathbf{v} \mid \mathbf{v} = \{v_i\} \text{ is a grid function on } \bar{\omega}_h \text{ and } v_i = 0 \text{ if } i = 0, N\}.$$

Based on the above lemmas, we will give some other lemmas and corollaries, which are important properties to proof the stability and the convergence of the implicit difference scheme (2.4).

**Lemma 2.6.** *For  $0 < \alpha < 1$ , and any  $\mathbf{v} \in V_h$ , it holds that*

$$(\delta_{x,+}^\alpha \mathbf{v}, \mathbf{v}) = (\delta_{x,-}^\alpha \mathbf{v}, \mathbf{v}) \geq \left( \frac{1}{h^\alpha} \sum_{k=0}^{N-1} \omega_k^{(\alpha)} \right) \|\mathbf{v}\|^2.$$

*Proof.* According to the discrete definitions of  $\delta_{x,+}^\alpha$  and  $\delta_{x,-}^\alpha$ , and  $v_0 = v_N = 0$ , we have

$$(\delta_{x,+}^\alpha \mathbf{v}, \mathbf{v}) = (\delta_{x,-}^\alpha \mathbf{v}, \mathbf{v})$$

and

$$\begin{aligned} (\delta_{x,+}^\alpha \mathbf{v}, \mathbf{v}) &= h^{1-\alpha} \sum_{i=1}^{N-1} \left( \sum_{k=0}^i \omega_k^{(\alpha)} v_{i-k+1} \right) v_i \\ &= \omega_1^{(\alpha)} h^{1-\alpha} \sum_{i=1}^{N-1} (v_i)^2 + (\omega_0^{(\alpha)} + \omega_2^{(\alpha)}) h^{1-\alpha} \sum_{i=1}^{N-2} v_i v_{i+1} + \sum_{k=3}^{N-1} \omega_k^{(\alpha)} h^{1-\alpha} \sum_{i=1}^{N-k} v_{i+k-1} v_i \\ &\geq \omega_1^{(\alpha)} h^{1-\alpha} \|\mathbf{v}\|^2 + (\omega_0^{(\alpha)} + \omega_2^{(\alpha)}) h^{1-\alpha} \sum_{i=1}^{N-2} \frac{(v_i)^2 + (v_{i+1})^2}{2} \\ &\quad + \sum_{k=3}^{N-1} \omega_k^{(\alpha)} h^{1-\alpha} \sum_{i=1}^{N-k} \frac{(v_{i+k-1})^2 + (v_i)^2}{2} \geq \left( \frac{1}{h^\alpha} \sum_{k=0}^{N-1} \omega_k^{(\alpha)} \right) \|\mathbf{v}\|^2. \end{aligned}$$

□

Further, the following conclusion holds.

**Corollary 1.** *For  $0 < \alpha < 1$ , and any  $\mathbf{v} \in V_h$ ,  $N \geq 2$ , there exists a positive constant  $c_1$ , such that*

$$(\delta_{x,+}^\alpha \mathbf{v}, \mathbf{v}) = (\delta_{x,-}^\alpha \mathbf{v}, \mathbf{v}) > c_1 \ln 2 \|\mathbf{v}\|^2.$$

*Proof.* Since

$$\sum_{k=N}^{2N+2} \omega_k^{(\alpha)} = \sum_{k=N}^{2N} g_k^{(\alpha)} + \frac{2-\alpha}{2} g_{N-1}^{(\alpha)} + \frac{\alpha}{2} g_{2N+2}^{(\alpha)} + g_{2N+1}^{(\alpha)}.$$

By Lemma 2.2, the following inequality is established:

$$\sum_{k=N}^{2N+2} \omega_k^{(\alpha)} < \sum_{k=N}^{2N} g_k^{(\alpha)},$$

when  $N \geq 2$ .

Then, by Lemma 2.2 and Lemma 2.4, there exist two positive constants  $\tilde{c}_1$  and  $c_1$ , such that

$$\begin{aligned} \frac{1}{h^\alpha} \sum_{k=N}^{\infty} \left( -\omega_k^{(\alpha)} \right) &> \frac{1}{h^\alpha} \sum_{k=N}^{2N+2} \left( -\omega_k^{(\alpha)} \right) > \frac{1}{h^\alpha} \sum_{k=N}^{2N} \left( -g_k^{(\alpha)} \right) \\ &\geq \tilde{c}_1 \sum_{k=N}^{2N} k^{-(\alpha+1)} N^\alpha > \tilde{c}_1 \sum_{k=N}^{2N} k^{-(\alpha+1)} \left( \frac{k}{2} \right)^\alpha \\ &= \frac{\tilde{c}_1}{2^\alpha} \sum_{k=N}^{2N} \frac{1}{k} > c_1 \int_N^{2N+1} \frac{1}{x} dx \geq c_1 \int_N^{2N} \frac{1}{x} dx = c_1 \ln 2, \quad N \geq 2. \end{aligned}$$

Here, the penultimate and antepenult inequalities are true due to the fact that  $J_1(x) = 1/x$  is a lower convex function and  $J_2(x) = \ln(x) > 0$ ,  $x \in [N, 2N + 1]$  is an increasing function.

Using Lemma 2.4 and Lemma 2.6, we obtain

$$(\delta_{x,+}^\alpha \mathbf{v}, \mathbf{v}) = (\delta_{x,-}^\alpha \mathbf{v}, \mathbf{v}) \geq \frac{1}{h^\alpha} \sum_{k=N}^{\infty} \left( -\omega_k^{(\alpha)} \right) \|\mathbf{v}\|^2 > c_1 \ln 2 \|\mathbf{v}\|^2.$$

□

Using the same argument as in the proof of Corollary 1, we can easily carry out the following corollary.

**Corollary 2.** (1) For  $1 < \beta < 2$ , and any  $\mathbf{v} \in V_h$ , it holds that

$$(\delta_{x,+}^\beta \mathbf{v}, \mathbf{v}) = (\delta_{x,-}^\beta \mathbf{v}, \mathbf{v}) \leq \left( \frac{1}{h^\beta} \sum_{k=0}^{N-1} \omega_k^{(\beta)} \right) \|\mathbf{v}\|^2.$$

(2) For  $1 < \beta < 2$ , and any  $\mathbf{v} \in V_h$ ,  $N \geq 3$ , there exists a positive constant  $c_2$ , such that

$$(-\delta_{x,+}^\beta \mathbf{v}, \mathbf{v}) = (-\delta_{x,-}^\beta \mathbf{v}, \mathbf{v}) > c_2 \ln 2 \|\mathbf{v}\|^2.$$

With the help of the preceding lemmas and corollaries, we can now establish the following theorem, which is essential for analyzing the stability of the proposed implicit difference scheme.

**Theorem 2.1.** For any  $\mathbf{v} \in V_h$ , it holds that

$$(\delta_h^{\alpha,\beta} \mathbf{v}, \mathbf{v}) \leq -c \ln 2 \|\mathbf{v}\|^2,$$

where  $c$  is a positive constant independent of the spatial step size  $h$ .

*Proof.* The concrete expression of  $(\delta_h^{\alpha,\beta} \mathbf{v}, \mathbf{v})$  can be written as

$$(\delta_h^{\alpha,\beta} \mathbf{v}, \mathbf{v}) = -d_+^{j+\sigma}(\delta_{x,+}^\alpha \mathbf{v}, \mathbf{v}) - d_-^{j+\sigma}(\delta_{x,-}^\alpha \mathbf{v}, \mathbf{v}) + e_+^{j+\sigma}(\delta_{x,+}^\beta \mathbf{v}, \mathbf{v}) + e_-^{j+\sigma}(\delta_{x,-}^\beta \mathbf{v}, \mathbf{v}).$$

According to Corollaries 1-2, there exists positive constants  $c_1$  and  $c_2$  independent of the spatial step size  $h$ , such that for any non-vanishing vector  $\mathbf{v} \in V_h$ , we have

$$\begin{aligned} (\delta_h^{\alpha,\beta} \mathbf{v}, \mathbf{v}) &= -d_+^{j+\sigma}(\delta_{x,+}^\alpha \mathbf{v}, \mathbf{v}) - d_-^{j+\sigma}(\delta_{x,-}^\alpha \mathbf{v}, \mathbf{v}) + e_+^{j+\sigma}(\delta_{x,+}^\beta \mathbf{v}, \mathbf{v}) + e_-^{j+\sigma}(\delta_{x,-}^\beta \mathbf{v}, \mathbf{v}) \\ &< -\ln 2 \left[ c_1(d_+^{j+\sigma} + d_-^{j+\sigma}) + c_2(e_+^{j+\sigma} + e_-^{j+\sigma}) \right] \|\mathbf{v}\|^2. \end{aligned}$$

For simplicity, we may take  $c = c_1(d_+^{j+\sigma} + d_-^{j+\sigma}) + c_2(e_+^{j+\sigma} + e_-^{j+\sigma})$ . Hence, the targeted result is immediately completed.  $\square$

**Remark.** *Proceeding as in the proof of Theorem 2.1, we can easily find that when the diffusion coefficients become  $d_\pm(x, t) > 0$  and  $e_\pm(x, t) > 0$  and satisfy*

$$d_+(x, t) + d_-(x, t) > k_1 > 0, \quad e_+(x, t) + e_-(x, t) > k_2 > 0.$$

*The conclusion of Theorem 2.1 is still valid, here we only let  $c = c_1 k_1 + c_2 k_2$  in the above proof.*

We also need another lemma, which had been proved by Alikhanov, to prove the stability and convergence of the implicit difference scheme, see [50] for details.

**Lemma 2.7.** [50] *Let  $V_\tau = \{\mathbf{u} \mid \mathbf{u} = (u^0, u^1, \dots, u^M)\}$ . For any  $\mathbf{u} \in V_\tau$ , one has the following inequality*

$$\left[ \sigma u^{j+1} + (1 - \sigma) u^j \right] \Delta_{0,t_{j+\sigma}}^\theta \mathbf{u} \geq \frac{1}{2} \Delta_{0,t_{j+\sigma}}^\theta (\mathbf{u})^2.$$

Now we can proof the stability and convergence of the implicit difference scheme (2.4). For convenience, in our proof, we denote  $q_s^{j+1} = \frac{\tau^{-\theta} c_{j-s}^{(\theta, \sigma)}}{\Gamma(2-\theta)}$ . Then  $\Delta_{0,t_{j+\sigma}}^\theta = \sum_{s=0}^j (u^{s+1} - u^s) q_s^{j+1}$ .

**Theorem 2.2.** *Denote  $u^{j+1} = (u_1^{j+1}, u_2^{j+1}, \dots, u_{N-1}^{j+1})^T$  and  $\|f^{j+\sigma}\|^2 = h \sum_{i=1}^{N-1} f^2(x_i, t_{j+\sigma})$ . Then the implicit difference scheme (2.4) is unconditionally stable for  $N \geq 3$ , and the following a priori estimate holds:*

$$\|u^{j+1}\|^2 \leq \|u^0\|^2 + \frac{T^\theta \Gamma(1-\theta)}{c \ln 2} \|f^{j+\sigma}\|^2, \quad 0 \leq j \leq M-1. \quad (2.5)$$

*Proof.* Taking the inner product of (2.4) with  $u^{(\sigma)}$ , we have

$$(\Delta_{0,t_{j+\sigma}}^\theta u, u^{(\sigma)}) = (\delta_h^{\alpha,\beta} u^{(\sigma)}, u^{(\sigma)}) + (f^{j+\sigma}, u^{(\sigma)}).$$

Using Theorem 2.1 and Lemma 2.7 obtains

$$\frac{1}{2} \Delta_{0,t_{j+\sigma}}^\theta \|u\|^2 \leq -c \ln 2 \left\| u^{(\sigma)} \right\|^2 + \varepsilon \left\| u^{(\sigma)} \right\|^2 + \frac{1}{4\varepsilon} \|f^{j+\sigma}\|^2, \quad \varepsilon > 0. \quad (2.6)$$

From (2.6), at  $\varepsilon = c \ln 2$  we get

$$\frac{1}{2} \Delta_{0,t_j+\sigma}^\theta \|u\|^2 \leq \frac{1}{4c \ln 2} \|f^{j+\sigma}\|^2. \quad (2.7)$$

Let us rewrite inequality (2.7) in the form

$$q_j^{j+1} \|u^{j+1}\|^2 \leq \sum_{s=1}^j (q_s^{j+1} - q_{s-1}^{j+1}) \|u^s\|^2 + q_0^{j+1} \|u^0\|^2 + \frac{1}{2c \ln 2} \|f^{j+\sigma}\|^2.$$

Noticing that  $q_0^{j+1} > \frac{1}{2T^\theta \Gamma(1-\theta)}$  (cf. [54]), we get

$$q_j^{j+1} \|u^{j+1}\|^2 \leq \sum_{s=1}^j (q_s^{j+1} - q_{s-1}^{j+1}) \|u^s\|^2 + q_0^{j+1} \left( \|u^0\|^2 + \frac{T^\theta \Gamma(1-\theta)}{c \ln 2} \|f^{j+\sigma}\|^2 \right). \quad (2.8)$$

Suppose  $h < 1$  and denote

$$\tilde{E} = \|u^0\|^2 + \frac{T^\theta \Gamma(1-\theta)}{c \ln 2} \|f^{j+\sigma}\|^2.$$

The inequality (2.8) is reduced to

$$q_j^{j+1} \|u^{j+1}\|^2 \leq \sum_{s=1}^j (q_s^{j+1} - q_{s-1}^{j+1}) \|u^s\|^2 + q_0^{j+1} \tilde{E}. \quad (2.9)$$

It is obvious that at  $j = 0$  the priori estimate (2.5) follows from (2.9). Let us prove that (2.5) holds for  $j = 1, 2, \dots, M-1$  by using the mathematical induction method. Let us assume that the inequality (2.5) takes place for all  $j = 0, 1, \dots, k-1$ :

$$\|u^{j+1}\|^2 \leq \tilde{E}, \quad j = 0, 1, \dots, k-1.$$

From (2.9) at  $j = k$  one has

$$\begin{aligned} q_k^{k+1} \|u^{k+1}\|^2 &\leq \sum_{s=1}^k (q_s^{k+1} - q_{s-1}^{k+1}) \|u^s\|^2 + q_0^{k+1} \tilde{E} \\ &\leq \sum_{s=1}^k (q_s^{k+1} - q_{s-1}^{k+1}) \tilde{E} + q_0^{k+1} \tilde{E} = q_k^{k+1} \tilde{E}. \end{aligned}$$

The proof of Theorem 2.2 is completed.  $\square$

With the above proof, the convergence of the implicit difference scheme (2.4) is easy to obtain.

**Theorem 2.3.** *Suppose that  $u(x, t)$  is the solution of (1.1) and  $\{u_i^j \mid x_i \in \bar{\omega}_h, 0 \leq j \leq M\}$  is the solution of the implicit difference scheme (2.4). Denote*

$$\xi_i^j = u(x_i, t_j) - u_i^j, \quad x_i \in \bar{\omega}_h, \quad 0 \leq j \leq M.$$

*Then there exists a positive constant  $\tilde{c}$  such that*

$$\|\xi^j\| \leq \tilde{c}(\tau^2 + h^2), \quad 0 \leq j \leq M.$$

*Proof.* It can easily obtain that  $\xi^j$  satisfies the following error equation

$$\begin{cases} \Delta_{0,t_j+\sigma}^\theta \xi_i = \delta_h^{\alpha,\theta} \xi_i^{(\sigma)} + R_i^{j+\sigma}, & 1 \leq i \leq N-1, \quad 0 \leq j \leq M-1, \\ \xi_i^0 = 0, & 1 \leq i \leq N-1, \\ \xi_0^j = \xi_N^j = 0, & 0 \leq j \leq M, \end{cases}$$

where  $R_i^{j+\sigma} = \mathcal{O}(\tau^2 + h^2)$ . By exploiting Theorem 2.2 we get

$$\|\xi^{j+1}\|^2 = \frac{T^\theta \Gamma(1-\theta)}{c \ln 2} \|R^{j+\sigma}\|^2 \leq \tilde{c}(\tau^2 + h^2), \quad 0 \leq j \leq M-1,$$

which implies the convergence in the mesh  $L_2$ -norm with rate  $\mathcal{O}(\tau^2 + h^2)$ .  $\square$

The unconditionally stability and convergence of IDS (2.4) have been proved, and some numerical tests are displayed to verify our results, in Section 4. In next section, we will discuss three fast solution techniques based on preconditioned iterative solvers to solve (2.4).

### 3 Fast implementation of IDM with the circulant preconditioner

Before moving into the investigation of fast solution techniques, the matrix form of implicit difference scheme (2.4) must be established first. In order to facilitate our discussion, we use notations in Section 2. Then, the matrix form of (2.4) corresponding to each time layer  $j$  can be written as follows:

$$\begin{aligned} \mathcal{M}^{j+\sigma} u^{j+1} &= B^{j+\sigma} u^j - \frac{\tau^{-\theta}}{\Gamma(2-\theta)} \sum_{s=0}^{j-1} c_{j-s}^{(\theta,\sigma)} (u^{s+1} - u^s) \\ &+ f^{j+\sigma}, \quad 0 \leq j \leq M-1, \end{aligned} \quad (3.1)$$

we assume that the sums to be equal to zero if the upper summation index is less than the lower one, where

$$\begin{aligned} \mathcal{M}^{j+\sigma} &= \frac{\tau^{-\theta}}{\Gamma(2-\theta)} c_0^{(\theta,\sigma)} I + \sigma \left( \frac{d_+^{j+\sigma}}{h^\alpha} A_\alpha + \frac{d_-^{j+\sigma}}{h^\alpha} A_\alpha^T - \frac{e_+^{j+\sigma}}{h^\beta} A_\beta - \frac{e_-^{j+\sigma}}{h^\beta} A_\beta^T \right), \\ B^{j+\sigma} &= \frac{\tau^{-\theta}}{\Gamma(2-\theta)} c_0^{(\theta,\sigma)} I + (1-\sigma) \left( \frac{d_+^{j+\sigma}}{h^\alpha} A_\alpha + \frac{d_-^{j+\sigma}}{h^\alpha} A_\alpha^T - \frac{e_+^{j+\sigma}}{h^\beta} A_\beta - \frac{e_-^{j+\sigma}}{h^\beta} A_\beta^T \right), \end{aligned}$$

and  $I$  is an identity matrix of order  $N-1$ , the two matrices  $A_\alpha$  and  $A_\beta$  are defined by

$$A_\alpha = \begin{bmatrix} \omega_1^{(\alpha)} & \omega_0^{(\alpha)} & & & \\ \omega_2^{(\alpha)} & \omega_1^{(\alpha)} & \omega_0^{(\alpha)} & & \\ \vdots & \ddots & \ddots & \ddots & \\ \omega_{N-2}^{(\alpha)} & \cdots & \ddots & \ddots & \omega_0^{(\alpha)} \\ \omega_{N-1}^{(\alpha)} & \omega_{N-2}^{(\alpha)} & \cdots & \omega_2^{(\alpha)} & \omega_1^{(\alpha)} \end{bmatrix}, \quad A_\beta = \begin{bmatrix} \omega_1^{(\beta)} & \omega_0^{(\beta)} & & & \\ \omega_2^{(\beta)} & \omega_1^{(\beta)} & \omega_0^{(\beta)} & & \\ \vdots & \ddots & \ddots & \ddots & \\ \omega_{N-2}^{(\beta)} & \cdots & \ddots & \ddots & \omega_0^{(\beta)} \\ \omega_{N-1}^{(\beta)} & \omega_{N-2}^{(\beta)} & \cdots & \omega_2^{(\beta)} & \omega_1^{(\beta)} \end{bmatrix}.$$

It is apparent that  $A_\alpha$  and  $A_\beta$  are Toeplitz matrices. Therefore, they can be stored with  $2N + 2$  entries. Krylov subspace methods with suitable circulant preconditioners [43, 55] can be used to efficiently solve Toeplitz or Toeplitz-like linear systems with a fast convergence rate. In this case, it is also remarked that the algorithmic complexity of preconditioned Krylov subspace methods is only in  $\mathcal{O}(N \log N)$  arithmetic operations per iteration step.

Inspired by the above consideration, we propose a circulant preconditioner to solve (3.1), which is generated from the Strang's circulant preconditioner [56], through three preconditioned Krylov subspace methods. The Strang's circulant matrix  $s(Q) = [s_{j-k}]_{0 \leq j, k < N}$  for a real Toeplitz matrix  $Q = [q_{j-k}]_{0 \leq j, k < N}$  is obtained by copying the central diagonals of  $Q$  and bringing them around to complete the circulant requirement. More precisely, the diagonals of  $s(Q)$  are given by

$$s_j = \begin{cases} q_j, & 0 \leq j < N/2, \\ 0, & j = N/2 \text{ if } N \text{ is even,} \\ q_{j-N}, & N/2 < j < N, \\ s_{j+N}, & 0 < -j < N. \end{cases}$$

Then our circulant preconditioner is defined as

$$P^{(j+\sigma)} = \begin{cases} \frac{\tau^{-\theta}}{\Gamma(2-\theta)} a_0^{(\theta, \sigma)} I + \sigma \left( \frac{d_+^{j+\sigma}}{h^\alpha} s(A_\alpha) + \frac{d_-^{j+\sigma}}{h^\alpha} s(A_\alpha^T) \right. \\ \quad \left. - \frac{e_+^{j+\sigma}}{h^\beta} s(A_\beta) - \frac{e_-^{j+\sigma}}{h^\beta} s(A_\beta^T) \right), & j = 0, \\ \frac{\tau^{-\theta}}{\Gamma(2-\theta)} (a_0^{(\theta, \sigma)} + b_1^{(\theta, \sigma)}) I + \sigma \left( \frac{d_+^{j+\sigma}}{h^\alpha} s(A_\alpha) + \frac{d_-^{j+\sigma}}{h^\alpha} s(A_\alpha^T) \right. \\ \quad \left. - \frac{e_+^{j+\sigma}}{h^\beta} s(A_\beta) - \frac{e_-^{j+\sigma}}{h^\beta} s(A_\beta^T) \right), & j = 1, \dots, M-1, \end{cases} \quad (3.2)$$

where the first columns of  $s(A_\gamma)$  and  $s(A_\gamma^T)$  ( $\gamma = \alpha, \beta$ ) are given by

$$\begin{bmatrix} \omega_1^{(\gamma)} \\ \vdots \\ \omega_{\lfloor \frac{N}{2} \rfloor}^{(\gamma)} \\ 0 \\ \vdots \\ 0 \\ \omega_0^{(\gamma)} \end{bmatrix} \text{ and } \begin{bmatrix} \omega_1^{(\gamma)} \\ \omega_0^{(\gamma)} \\ 0 \\ \vdots \\ 0 \\ \omega_{\lfloor \frac{N}{2} \rfloor}^{(\gamma)} \\ \vdots \\ \omega_2^{(\gamma)} \end{bmatrix}, \text{ respectively.}$$

To make sure the preconditioner defined in (3.2) is well-defined, let us illustrate that  $P^{(j+\sigma)}$  are nonsingular. Before that, we need to give the following theorem, which is essential to check the nonsingularity of  $P^{(j+\sigma)}$ .

- Theorem 3.1.** 1. The real parts of all eigenvalues of  $s(A_\alpha)$  and  $s(A_\alpha^T)$  are strictly positive for all  $N$ ;  
 2. The real parts of all eigenvalues of  $s(A_\beta)$  and  $s(A_\beta^T)$  are strictly negative for all  $N$ .

*Proof.* Firstly, we proof the real parts of all eigenvalues of  $s(A_\alpha)$  are strictly positive for all  $N$ .

Recall that the real parts of all eigenvalues of  $s(A_\alpha)$  are equivalent to the eigenvalues of  $\frac{s(A_\alpha)+[s(A_\alpha)]^*}{2}$  (where  $S^*$  represents conjugate transpose of matrix  $S$ ). Therefore, it is sufficient to show that all eigenvalues of  $\frac{s(A_\alpha)+s^*(A_\alpha)}{2}$  are strictly positive for all  $N$ .

According to Gershgrin's theorem [57], all the Gershgrin disc of the circulant matrix  $\frac{s(A_\alpha)+s^*(A_\alpha)}{2}$  are centered at  $\omega_1^{(\alpha)} > 0$  with radius

$$r_\alpha = - \sum_{k=0, k \neq 1}^{\lfloor \frac{N}{2} \rfloor} \omega_k^{(\alpha)} < - \sum_{k=0, k \neq 1}^{\infty} \omega_k^{(\alpha)} = \omega_1^{(\alpha)},$$

by the Lemma 2.4, the first part of this theorem is proved.

Then, we prove the second part of the theorem. Similarly, all the Gershgrin disc of the circulant matrix  $\frac{s(A_\beta)+s^*(A_\beta)}{2}$  are centered at  $\omega_1^{(\beta)} < 0$  with radius

$$r_\beta = \sum_{k=0, k \neq 1}^{\lfloor \frac{N}{2} \rfloor} \omega_k^{(\beta)} < \sum_{k=0, k \neq 1}^{\infty} \omega_k^{(\beta)} = -\omega_1^{(\beta)},$$

by the Lemma 2.5, the second part of this theorem is proved. Finally, we complete the proof of the theorem.  $\square$

With the help of Theorem 3.1, we will check the circulant preconditioners  $P^{(j+\sigma)}$  are non-singular.

**Theorem 3.2.** *The circulant preconditioners  $P^{(j+\sigma)}$  defined in (3.2) are nonsingular.*

*Proof.* As we know, a circulant matrix can be diagonalized by the Fourier matrix  $F$  [56]. Then it follows that  $s(A_\gamma) = F^* \Lambda_\gamma F$ ,  $s(A_\gamma^T) = F^* \bar{\Lambda}_\gamma F$ , where  $\gamma = \alpha, \beta$ , and  $\bar{\Lambda}_\gamma$  is the complex conjugate of  $\Lambda_\gamma$ . Decompose the circulant matrix  $P^{(j+\sigma)} = F^* \Lambda_P F$  with the diagonal matrix

$$\Lambda_P = \begin{cases} \frac{\tau^{-\theta}}{\Gamma(2-\theta)} a_0^{(\theta, \sigma)} I + \sigma \left( \frac{d_+^{j+\sigma}}{h^\alpha} \Lambda_\alpha + \frac{d_-^{j+\sigma}}{h^\alpha} \bar{\Lambda}_\alpha \right. \\ \quad \left. - \frac{e_+^{j+\sigma}}{h^\beta} \Lambda_\beta - \frac{e_-^{j+\sigma}}{h^\beta} \bar{\Lambda}_\beta \right), & j = 0, \\ \frac{\tau^{-\theta}}{\Gamma(2-\theta)} (a_0^{(\theta, \sigma)} + b_1^{(\theta, \sigma)}) I + \sigma \left( \frac{d_+^{j+\sigma}}{h^\alpha} \Lambda_\alpha + \frac{d_-^{j+\sigma}}{h^\alpha} \bar{\Lambda}_\alpha \right. \\ \quad \left. - \frac{e_+^{j+\sigma}}{h^\beta} \Lambda_\beta - \frac{e_-^{j+\sigma}}{h^\beta} \bar{\Lambda}_\beta \right), & j = 1, \dots, M-1. \end{cases}$$

Then the real part of  $\Lambda_P$  can be written as

$$Re([\Lambda_P]_{k,k}) = \begin{cases} \frac{\tau^{-\theta}}{\Gamma(2-\theta)} a_0^{(\theta, \sigma)} + \sigma \left( \frac{d_+^{j+\sigma}}{h^\alpha} Re([\Lambda_\alpha]_{k,k}) + \frac{d_-^{j+\sigma}}{h^\alpha} Re([\bar{\Lambda}_\alpha]_{k,k}) \right. \\ \quad \left. - \frac{e_+^{j+\sigma}}{h^\beta} Re([\Lambda_\beta]_{k,k}) - \frac{e_-^{j+\sigma}}{h^\beta} Re([\bar{\Lambda}_\beta]_{k,k}) \right), & j = 0, \\ \frac{\tau^{-\theta}}{\Gamma(2-\theta)} (a_0^{(\theta, \sigma)} + b_1^{(\theta, \sigma)}) + \sigma \left( \frac{d_+^{j+\sigma}}{h^\alpha} Re([\Lambda_\alpha]_{k,k}) + \frac{d_-^{j+\sigma}}{h^\alpha} Re([\bar{\Lambda}_\alpha]_{k,k}) \right. \\ \quad \left. - \frac{e_+^{j+\sigma}}{h^\beta} Re([\Lambda_\beta]_{k,k}) - \frac{e_-^{j+\sigma}}{h^\beta} Re([\bar{\Lambda}_\beta]_{k,k}) \right), & j = 1, \dots, M-1. \end{cases}$$

Combining Theorem 3.1, we obtain

$$Re([\Lambda_P]_{k,k}) > 0.$$

Consequently,  $P^{(j+\sigma)}$  are invertible.  $\square$

Unfortunately, due to the properties of coefficients  $\omega_k^{(\alpha)}$  and  $\omega_k^{(\beta)}$ , it is difficult to theoretically investigate the eigenvalue distributions of preconditioned matrix  $(P^{(j+\sigma)})^{-1}\mathcal{M}^{j+\sigma}$ , but we still can give some figures to illustrate the clustering eigenvalue distributions of several specified preconditioned matrices in next section.

## 4 Numerical results

In this section, we carry out several numerical experiments, which are given in Examples 1-2, to illustrate that our proposed IDM can indeed convergent with second order accuracy in both space and time. Some other numerical experiments, given in Examples 3-4, are reported to illustrate the effectiveness of the fast solution techniques. For direct solver, we choose LU factorization of MATLAB in Examples 3-4, and its CPU time is represented. For three Krylov subspace methods (BiCGSTAB, BiCRSTAB and GPBiCOR( $m, \ell$ )) with circulant preconditioners, number of iterations required for convergence and CPU time of those methods are reported. Furthermore, we denote PBiCGSTAB, PBiCRSTAB and PGPBiCOR( $m, \ell$ ) as the preconditioned version of BiCGSTAB, BiCRSTAB and GPBiCOR( $m, \ell$ ), respectively. The stopping criterion of those methods is

$$\frac{\|r^{(k)}\|_2}{\|r^{(0)}\|_2} < 10^{-12},$$

where  $r^{(k)}$  is the residual vector of the linear system after  $k$  iterations, and the initial guess at each time step is chosen as the zero vector. All experiments were performed on a Windows 7 (32 bit) PC-Intel(R) Core(TM) i3-2130 CPU 3.40GHz, 4GB of RAM using MATLAB R2015b.

**Example 1.** In this example, we consider the equation (1.1) on space interval  $[0, L] = [0, 1]$  and time interval  $[0, T] = [0, 1]$  with advection coefficients  $d_+(t) = d_+$ ,  $d_-(t) = d_-$ , diffusion coefficients  $e_+(t) = e_+$ ,  $e_-(t) = e_-$ , and source term

$$\begin{aligned} f(x, t) = & \frac{\Gamma(3+\theta)}{\Gamma(3)} t^2 x^2 (1-x)^2 + t^{2+\theta} \left\{ \frac{\Gamma(3)}{\Gamma(3-\alpha)} [d_+ x^{2-\alpha} + d_- (1-x)^{2-\alpha}] \right. \\ & - \frac{2\Gamma(4)}{\Gamma(4-\alpha)} [d_+ x^{3-\alpha} + d_- (1-x)^{3-\alpha}] + \frac{\Gamma(5)}{\Gamma(5-\alpha)} [d_+ x^{4-\alpha} + d_- (1-x)^{4-\alpha}] \left. \right\} \\ & - t^{2+\theta} \left\{ \frac{\Gamma(3)}{\Gamma(3-\beta)} [e_+ x^{2-\beta} + e_- (1-x)^{2-\beta}] - \frac{2\Gamma(4)}{\Gamma(4-\beta)} [e_+ x^{3-\beta} + e_- (1-x)^{3-\beta}] \right. \\ & \left. + \frac{\Gamma(5)}{\Gamma(5-\beta)} [e_+ x^{4-\beta} + e_- (1-x)^{4-\beta}] \right\}. \end{aligned}$$

The exact solution is  $u(x, t) = t^{2+\theta} x^2 (1-x)^2$ . For the finite difference discretization, the space step and time step are taken to be  $h = 1/N$  and  $\tau = h$ , respectively. The errors

Table 1:  $L_2$ -norm and maximum norm error behavior versus  $\tau$ -grid size reduction when  $\alpha = 0.6$ ,  $\beta = 1.8$ ,  $d_+ = 10$ ,  $d_- = 11$ ,  $e_+ = 1e - 11$ ,  $e_- = 1e - 12$  and  $h = 1/3000$  in Example 1.

$\theta$	$\tau$	$\ \xi\ _{\mathcal{C}(\bar{\omega}_{h\tau})}$	CO in $\ \cdot\ _{\mathcal{C}(\bar{\omega}_{h\tau})}$	$\max_{0 \leq n \leq M} \ \xi^n\ _0$	CO in $\ \cdot\ _0$
0.10	1/8	5.1122e-05	–	3.2467e-05	–
	1/16	1.2793e-05	1.9986	8.1264e-06	1.9983
	1/32	3.1906e-06	2.0035	2.0283e-06	2.0024
	1/64	7.8749e-07	2.0185	5.0230e-07	2.0136
	1/128	1.8710e-07	2.0734	1.2096e-07	2.0541
0.50	1/8	3.2725e-04	–	2.0791e-04	–
	1/16	8.2154e-05	1.9940	5.2193e-05	1.9940
	1/32	2.0568e-05	1.9979	1.3068e-05	1.9978
	1/64	5.1359e-06	2.0017	3.2645e-06	2.0011
	1/128	1.2740e-06	2.0112	8.1142e-07	2.0083
0.90	1/8	6.4147e-04	–	4.0767e-04	–
	1/16	1.6053e-04	1.9985	1.0202e-04	1.9986
	1/32	4.0133e-05	2.0000	2.5504e-05	2.0000
	1/64	1.0021e-05	2.0017	6.3696e-06	2.0015
	1/128	2.4943e-06	2.0063	1.5869e-06	2.0050
0.99	1/8	7.0327e-04	–	4.4702e-04	–
	1/16	1.7582e-04	1.9999	1.1176e-04	1.9999
	1/32	4.3946e-05	2.0003	2.7935e-05	2.0003
	1/64	1.0976e-05	2.0014	6.9786e-06	2.0011
	1/128	2.7340e-06	2.0053	1.7398e-06	2.0040

( $\xi = U - u$ ) and convergence order (CO) in the norms  $\|\cdot\|_0$  and  $\|\cdot\|_{\mathcal{C}(\bar{\omega}_{h\tau})}$ , where  $\|U\|_{\mathcal{C}(\bar{\omega}_{h\tau})} = \max_{(x_i, t_j) \in \bar{\omega}_{h\tau}} |U|$ , are given in Tables 1-4.

As can be seen in Table 1 and 3, when  $h = 1/3000$ , the maximum error decreases steadily with the shortening of time step, and the convergence order of time is the expected  $\mathcal{O}(\tau^2)$ , where the convergence order (CO) is given by the following formula:  $\text{CO} = \log_{\tau_1/\tau_2} \frac{\|\xi_1\|}{\|\xi_2\|}$  ( $\xi_i$  is the error corresponding to  $h_i$ ). On the other hand, Table 2 and 4 illustrate that if  $h = \tau$ , a reduction in the maximum error occurs along with the decrease of space step and time step, and the spatial convergence order is  $\mathcal{O}(h^2)$ , where the convergence order (CO) is given by the formula:  $\text{CO} = \log_{h_1/h_2} \frac{\|\xi_1\|}{\|\xi_2\|}$ . Figs. 1-2 are plotted to further explain the reliability of our proposed scheme, and indicate that the ‘quadratic-type’ order of accuracy can achieve the desired order  $\mathcal{O}(\tau^2 + h^2)$ .

Table 2:  $L_2$ -norm and maximum norm error behavior versus grid size reduction when  $\alpha = 0.6$ ,  $\beta = 1.8$ ,  $d_+ = 10$ ,  $d_- = 11$ ,  $e_+ = 1e - 11$ ,  $e_- = 1e - 12$  and  $\tau = h$  in Example 1.

$\theta$	$\tau$	$\ \xi\ _{\mathcal{C}(\bar{\omega}_{h\tau})}$	CO in $\ \cdot\ _{\mathcal{C}(\bar{\omega}_{h\tau})}$	$\max_{0 \leq n \leq M} \ \xi^n\ _0$	CO in $\ \cdot\ _0$
0.10	1/20	3.9523e-04	–	2.3180e-04	–
	1/40	1.2051e-04	1.7135	6.1600e-05	1.9119
	1/80	3.3072e-05	1.8655	1.6086e-05	1.9372
	1/160	8.6598e-06	1.9332	4.1448e-06	1.9564
	1/320	2.2169e-06	1.9658	1.0576e-06	1.9705
0.50	1/20	3.9330e-04	–	2.0870e-04	–
	1/40	1.1971e-04	1.7161	5.6407e-05	1.8875
	1/80	3.2868e-05	1.8648	1.4879e-05	1.9226
	1/160	8.6136e-06	1.9320	3.8579e-06	1.9474
	1/320	2.2069e-06	1.9646	9.8825e-07	1.9649
0.90	1/20	3.8941e-04	–	1.8407e-04	–
	1/40	1.1832e-04	1.7186	5.0980e-05	1.8522
	1/80	3.2522e-05	1.8632	1.3632e-05	1.9030
	1/160	8.5355e-06	1.9299	3.5627e-06	1.9359
	1/320	2.1899e-06	1.9626	9.1705e-07	1.9579
0.99	1/20	3.8810e-04	–	1.7924e-04	–
	1/40	1.1789e-04	1.7189	4.9922e-05	1.8441
	1/80	3.2418e-05	1.8626	1.3388e-05	1.8988
	1/160	8.5121e-06	1.9292	3.5048e-06	1.9335
	1/320	2.1849e-06	1.9620	9.0304e-07	1.9565

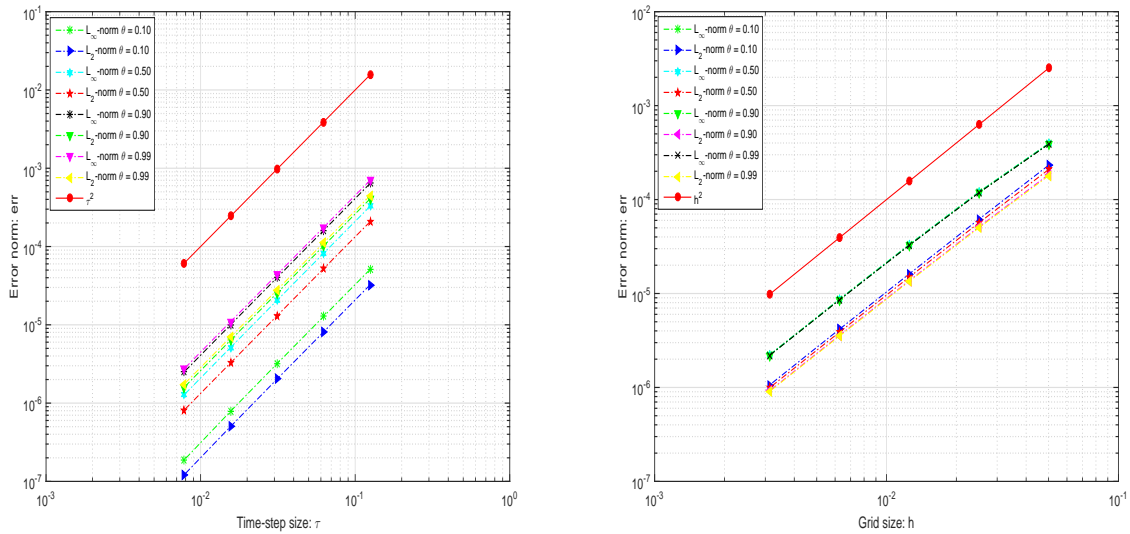


Fig. 1: Comparison the order of accuracy obtained by our proposed IDS for Example 1 in space and time variables. Left: time direction; Right: space direction.

Table 3:  $L_2$ -norm and maximum norm error behavior versus  $\tau$ -grid size reduction when  $\alpha = 0.99$ ,  $\beta = 1.99$ ,  $d_+ = 10$ ,  $d_- = 11$ ,  $e_+ = 1e - 11$ ,  $e_- = 1e - 12$  and  $h = 1/3000$  in Example 1.

$\theta$	$\tau$	$\ \xi\ _{C(\bar{\omega}_{h\tau})}$	CO in $\ \cdot\ _{C(\bar{\omega}_{h\tau})}$	$\max_{0 \leq n \leq M} \ \xi^n\ _0$	CO in $\ \cdot\ _0$
0.10	1/8	4.1937e-05	–	2.5736e-05	–
	1/16	1.0478e-05	2.0008	6.4294e-06	2.0011
	1/32	2.6020e-06	2.0097	1.5958e-06	2.0104
	1/64	6.3195e-07	2.0417	3.8698e-07	2.0440
	1/128	1.4591e-07	2.1147	8.9174e-08	2.1175
0.50	1/8	2.7287e-04	–	1.6767e-04	–
	1/16	6.8222e-05	1.9999	4.1899e-05	2.0006
	1/32	1.7015e-05	2.0035	1.0445e-05	2.0042
	1/64	4.2293e-06	2.0083	2.5949e-06	2.0090
	1/128	1.0391e-06	2.0251	6.3685e-07	2.0266
0.90	1/8	5.3810e-04	–	3.3051e-04	–
	1/16	1.3420e-04	2.0035	8.2395e-05	2.0040
	1/32	3.3422e-05	2.0055	2.0511e-05	2.0062
	1/64	8.3103e-06	2.0078	5.0974e-06	2.0085
	1/128	2.0564e-06	2.0148	1.2604e-06	2.0159
0.99	1/8	5.9293e-04	–	3.6428e-04	–
	1/16	1.4819e-04	2.0004	9.1037e-05	2.0005
	1/32	3.7019e-05	2.0012	2.2739e-05	2.0013
	1/64	9.2372e-06	2.0027	5.6732e-06	2.0029
	1/128	2.2960e-06	2.0084	1.4096e-06	2.0089

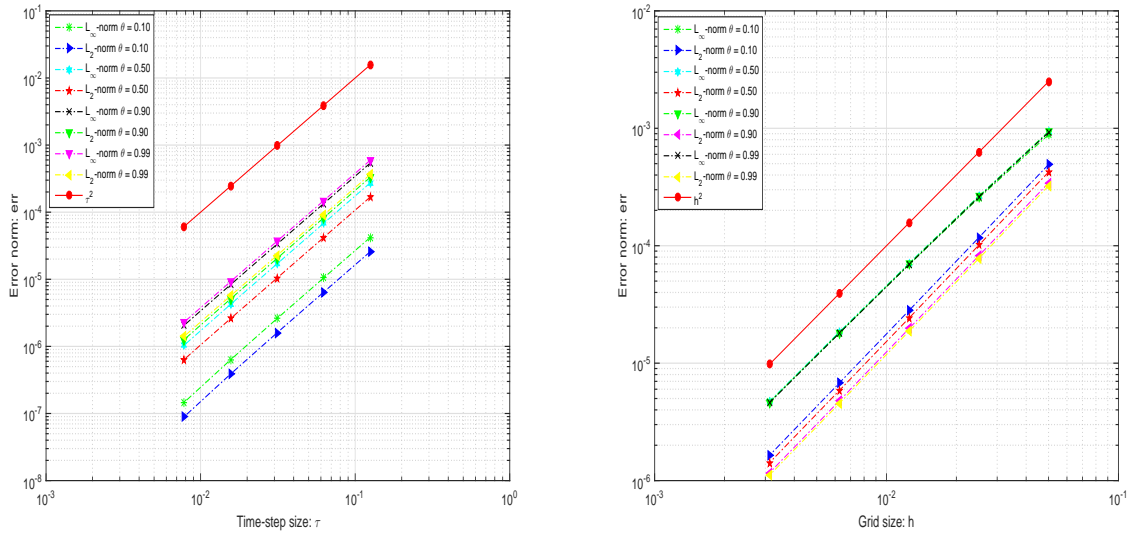


Fig. 2: Comparison the order of accuracy obtained by our proposed IDS for Example 1 in space and time variables. Left: time direction; Right: space direction.

**Example 2.** In this example, we consider that the diffusion coefficients are functions of  $x$  and

Table 4:  $L_2$ -norm and maximum norm error behavior versus grid size reduction when  $\alpha = 0.99$ ,  $\beta = 1.99$ ,  $d_+ = 10$ ,  $d_- = 11$ ,  $e_+ = 1e - 11$ ,  $e_- = 1e - 12$  and  $\tau = h$  in Example 1.

$\theta$	$\tau$	$\ \xi\ _{\mathcal{C}(\bar{\omega}_{h\tau})}$	CO in $\ \cdot\ _{\mathcal{C}(\bar{\omega}_{h\tau})}$	$\max_{0 \leq n \leq M} \ \xi^n\ _0$	CO in $\ \cdot\ _0$
0.10	1/20	8.8366e-04	–	4.9189e-04	–
	1/40	2.5507e-04	1.7926	1.1727e-04	2.0685
	1/80	6.8961e-05	1.8870	2.8081e-05	2.0622
	1/160	1.8070e-05	1.9322	6.7635e-06	2.0538
	1/320	4.6589e-06	1.9555	1.6376e-06	2.0462
0.50	1/20	9.3277e-04	–	4.2427e-04	–
	1/40	2.6451e-04	1.8182	1.0108e-04	2.0695
	1/80	7.0778e-05	1.9019	2.4196e-05	2.0626
	1/160	1.8414e-05	1.9425	5.8353e-06	2.0519
	1/320	4.7225e-06	1.9632	1.4167e-06	2.0423
0.90	1/20	9.4010e-04	–	3.4319e-04	–
	1/40	2.6393e-04	1.8326	8.2132e-05	2.0630
	1/80	7.0222e-05	1.9102	1.9700e-05	2.0597
	1/160	1.8198e-05	1.9481	4.7671e-06	2.0470
	1/320	4.6536e-06	1.9674	1.1632e-06	2.0350
0.99	1/20	9.2218e-04	–	3.2376e-04	–
	1/40	2.5952e-04	1.8292	7.7788e-05	2.0573
	1/80	6.9167e-05	1.9077	1.8694e-05	2.0570
	1/160	1.7949e-05	1.9462	4.5308e-06	2.0447
	1/320	4.5949e-06	1.9658	1.1076e-06	2.0323

$t$ , i.e., the diffusion coefficients  $d_{\pm}(t)$  and  $e_{\pm}(t)$  in (1.1) are replaced by  $d_{\pm}(x, t)$  and  $e_{\pm}(x, t)$ , respectively, which satisfy the conditions given in the Remark. Moreover,

$$\begin{aligned} d_+(x, t) &= 0.1(3 - x)e^t, & d_-(x, t) &= xe^{-t} + 0.5, \\ e_+(x, t) &= 0.1(2 - x)^2(1 + t)^2, & e_-(x, t) &= (1 + t^2) \cos x. \end{aligned}$$

Let  $L = 1$ ,  $T = 1$  and the exact solution  $u(x, t) = t^{2+\theta}x^2(1 - x)^2$ . Then, source term

$$\begin{aligned} f(x, t) &= \frac{\Gamma(3 + \theta)}{\Gamma(3)} t^2 x^2 (1 - x)^2 + t^{2+\theta} \left\{ \frac{\Gamma(3)}{\Gamma(3 - \alpha)} [d_+(x, t)x^{2-\alpha} + d_-(x, t)(1 - x)^{2-\alpha}] \right. \\ &\quad - \frac{2\Gamma(4)}{\Gamma(4 - \alpha)} [d_+(x, t)x^{3-\alpha} + d_-(x, t)(1 - x)^{3-\alpha}] + \frac{\Gamma(5)}{\Gamma(5 - \alpha)} [d_+(x, t)x^{4-\alpha} \\ &\quad \left. + d_-(x, t)(1 - x)^{4-\alpha}] \right\} - t^{2+\theta} \left\{ \frac{\Gamma(3)}{\Gamma(3 - \beta)} [e_+(x, t)x^{2-\beta} + e_-(x, t)(1 - x)^{2-\beta}] \right. \\ &\quad - \frac{2\Gamma(4)}{\Gamma(4 - \beta)} [e_+(x, t)x^{3-\beta} + e_-(x, t)(1 - x)^{3-\beta}] + \frac{\Gamma(5)}{\Gamma(5 - \beta)} [e_+(x, t)x^{4-\beta} \\ &\quad \left. + e_-(x, t)(1 - x)^{4-\beta}] \right\}. \end{aligned}$$

For the finite difference discretization, the space step and time step are taken to be  $h = 1/N$  and  $\tau = h$ , respectively. The errors ( $\xi = U - u$ ) and convergence order (CO) in the norms  $\|\cdot\|_0$  and  $\|\cdot\|_{\mathcal{C}(\bar{\omega}_{h\tau})}$  are given in Tables 5-8.

Table 6 and 8 show that when  $h = \tau$ , a reduction in the maximum error occurs along with the decrease of space step and time step, and the spatial convergence order is  $\mathcal{O}(h^2)$ , where the convergence order (CO) is given in Example 1. On the other hand, as seen from Table 5 and 7, if  $h = 1/3000$ , the maximum error decreases steadily with the shortening of time step, and the convergence order of time is the expected  $\mathcal{O}(\tau^2)$ , where the convergence order (CO) is given in Example 1. Figs. 3-4 are plotted to further illustrate the reliability of our proposed scheme, and indicate that the ‘quadratic-type’ order of accuracy is achieved both in time and space directions.

Table 5:  $L_2$ -norm and maximum norm error behavior versus  $\tau$ -grid size reduction when  $\alpha = 0.6$ ,  $\beta = 1.8$ , and  $h = 1/3000$  in Example 2.

$\theta$	$\tau$	$\ \xi\ _{\mathcal{C}(\bar{\omega}_{h\tau})}$	CO in $\ \cdot\ _{\mathcal{C}(\bar{\omega}_{h\tau})}$	$\max_{0 \leq n \leq M} \ \xi^n\ _0$	CO in $\ \cdot\ _0$
0.10	1/8	5.1069e-05	–	3.2414e-05	–
	1/16	1.2775e-05	1.9991	8.1085e-06	1.9991
	1/32	3.1811e-06	2.0057	2.0193e-06	2.0056
	1/64	7.8021e-07	2.0276	4.9554e-07	2.0268
	1/128	1.8119e-07	2.1064	1.1516e-07	2.1053
0.50	1/8	3.2669e-04	–	2.0744e-04	–
	1/16	8.2004e-05	1.9942	5.2066e-05	1.9943
	1/32	2.0525e-05	1.9983	1.3031e-05	1.9984
	1/64	5.1202e-06	2.0031	3.2508e-06	2.0031
	1/128	1.2654e-06	2.0166	8.0364e-07	2.0162
0.90	1/8	6.3996e-04	–	4.0647e-04	–
	1/16	1.6014e-04	1.9987	1.0170e-04	1.9988
	1/32	4.0027e-05	2.0003	2.5420e-05	2.0004
	1/64	9.9898e-06	2.0024	6.3441e-06	2.0025
	1/128	2.4820e-06	2.0090	1.5764e-06	2.0088
0.99	1/8	7.0163e-04	–	4.4572e-04	–
	1/16	1.7539e-04	2.0001	1.1142e-04	2.0001
	1/32	4.3834e-05	2.0005	2.7846e-05	2.0005
	1/64	1.0944e-05	2.0019	6.9524e-06	2.0019
	1/128	2.7216e-06	2.0076	1.7293e-06	2.0073

Table 6:  $L_2$ -norm and maximum norm error behavior versus grid size reduction when  $\alpha = 0.6$ ,  $\beta = 1.8$ , and  $\tau = h$  in Example 2.

$\theta$	$\tau$	$\ \xi\ _{\mathcal{C}(\bar{\omega}_{h\tau})}$	CO in $\ \cdot\ _{\mathcal{C}(\bar{\omega}_{h\tau})}$	$\max_{0 \leq n \leq M} \ \xi^n\ _0$	CO in $\ \cdot\ _0$
0.10	1/20	5.6748e-04	—	3.8266e-04	—
	1/40	1.3773e-04	2.0427	9.2099e-05	2.0548
	1/80	3.3326e-05	2.0472	2.2167e-05	2.0548
	1/160	8.0648e-06	2.0469	5.3436e-06	2.0525
	1/320	1.9525e-06	2.0463	1.2912e-06	2.0491
0.50	1/20	5.0695e-04	—	3.4348e-04	—
	1/40	1.2294e-04	2.0439	8.2540e-05	2.0571
	1/80	2.9672e-05	2.0507	1.9829e-05	2.0575
	1/160	7.1600e-06	2.0511	4.7722e-06	2.0549
	1/320	1.7288e-06	2.0502	1.1518e-06	2.0508
0.90	1/20	4.2958e-04	—	2.9232e-04	—
	1/40	1.0386e-04	2.0482	7.0165e-05	2.0587
	1/80	2.4990e-05	2.0553	1.6831e-05	2.0597
	1/160	6.0091e-06	2.0561	4.0466e-06	2.0563
	1/320	1.4455e-06	2.0556	9.7649e-07	2.0510
0.99	1/20	4.1111e-04	—	2.7989e-04	—
	1/40	9.9296e-05	2.0497	6.7179e-05	2.0588
	1/80	2.3872e-05	2.0564	1.6112e-05	2.0599
	1/160	5.7358e-06	2.0573	3.8740e-06	2.0563
	1/320	1.3783e-06	2.0571	9.3512e-07	2.0506

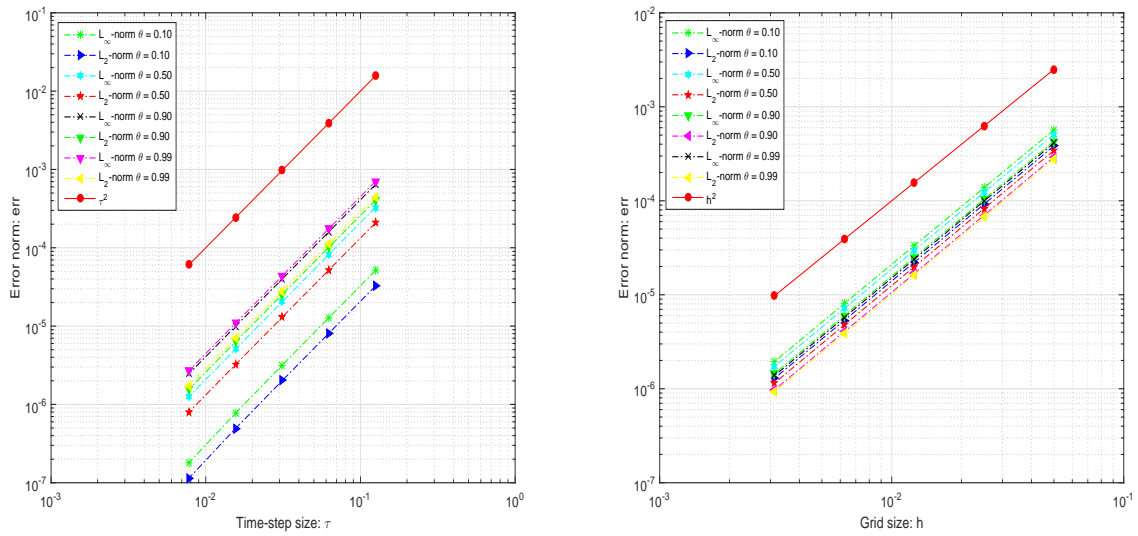


Fig. 3: Comparison the order of accuracy obtained by our proposed scheme for Example 2 in space and time variables. Left: time direction; Right: space direction.

Table 7:  $L_2$ -norm and maximum norm error behavior versus  $\tau$ -grid size reduction when  $\alpha = 0.99$ ,  $\beta = 1.99$ , and  $h = 1/3000$  in Example 2.

$\theta$	$\tau$	$\ \xi\ _{\mathcal{C}(\bar{\omega}_{h\tau})}$	CO in $\ \cdot\ _{\mathcal{C}(\bar{\omega}_{h\tau})}$	$\max_{0 \leq n \leq M} \ \xi^n\ _0$	CO in $\ \cdot\ _0$
0.10	1/8	5.1622e-05	—	3.2813e-05	—
	1/16	1.2909e-05	1.9996	8.2041e-06	1.9998
	1/32	3.2104e-06	2.0076	2.0387e-06	2.0087
	1/64	7.8313e-07	2.0354	4.9578e-07	2.0399
	1/128	1.8048e-07	2.1174	1.1369e-07	2.1246
0.50	1/8	3.2998e-04	—	2.0982e-04	—
	1/16	8.2843e-05	1.9939	5.2673e-05	1.9940
	1/32	2.0734e-05	1.9984	1.3181e-05	1.9986
	1/64	5.1690e-06	2.0041	3.2843e-06	2.0048
	1/128	1.2733e-06	2.0213	8.0755e-07	2.0240
0.90	1/8	6.4609e-04	—	4.1091e-04	—
	1/16	1.6170e-04	1.9985	1.0283e-04	1.9985
	1/32	4.0421e-05	2.0001	2.5704e-05	2.0003
	1/64	1.0086e-05	2.0027	6.4119e-06	2.0031
	1/128	2.5022e-06	2.0111	1.5892e-06	2.0125
0.99	1/8	7.0808e-04	—	4.5037e-04	—
	1/16	1.7700e-04	2.0002	1.1259e-04	2.0001
	1/32	4.4232e-05	2.0006	2.8133e-05	2.0007
	1/64	1.1039e-05	2.0024	7.0200e-06	2.0027
	1/128	2.7413e-06	2.0097	1.7418e-06	2.0109

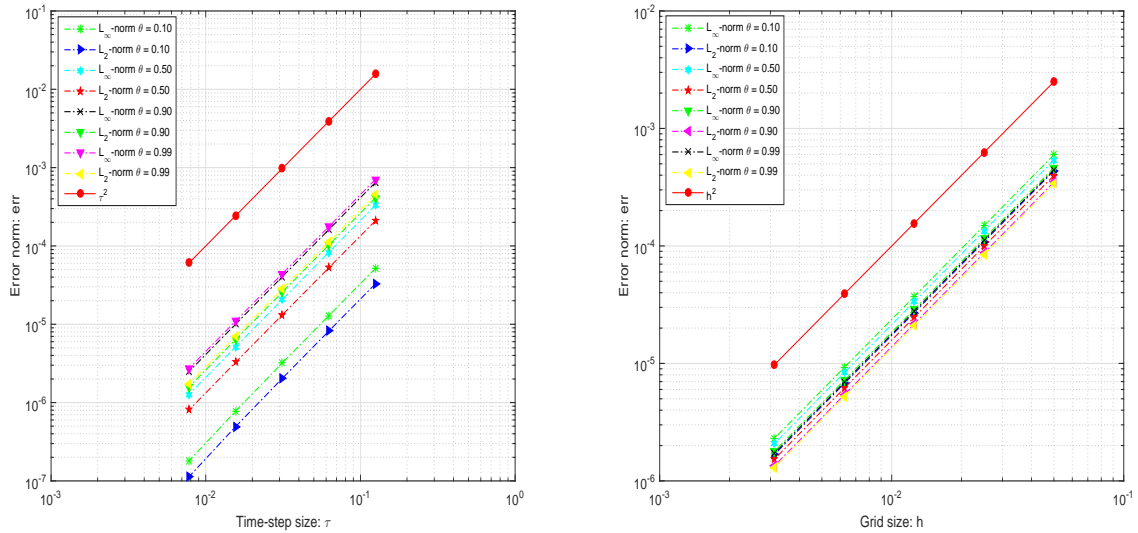


Fig. 4: Comparison the order of accuracy obtained by our proposed scheme for Example 2 in space and time variables. Left: time direction; Right: space direction.

**Example 3.** In this example, we consider the case of constant coefficients, and the exact solution

Table 8:  $L_2$ -norm and maximum norm error behavior versus grid size reduction when  $\alpha = 0.99$ ,  $\beta = 1.99$ , and  $\tau = h$  in Example 2.

$\theta$	$\tau$	$\ \xi\ _{\mathcal{C}(\bar{\omega}_{h\tau})}$	CO in $\ \cdot\ _{\mathcal{C}(\bar{\omega}_{h\tau})}$	$\max_{0 \leq n \leq M} \ \xi^n\ _0$	CO in $\ \cdot\ _0$
0.10	1/20	5.9678e-04	–	4.3572e-04	–
	1/40	1.4888e-04	2.0031	1.0863e-04	2.0040
	1/80	3.7129e-05	2.0035	2.7073e-05	2.0045
	1/160	9.2586e-06	2.0037	6.7465e-06	2.0047
	1/320	2.3087e-06	2.0037	1.6811e-06	2.0047
0.50	1/20	5.3818e-04	–	3.9798e-04	–
	1/40	1.3431e-04	2.0026	9.9253e-05	2.0035
	1/80	3.3492e-05	2.0036	2.4733e-05	2.0047
	1/160	8.3503e-06	2.0039	6.1620e-06	2.0050
	1/320	2.0818e-06	2.0040	1.5351e-06	2.0051
0.90	1/20	4.6347e-04	–	3.4940e-04	–
	1/40	1.1577e-04	2.0012	8.7204e-05	2.0024
	1/80	2.8872e-05	2.0035	2.1731e-05	2.0047
	1/160	7.1982e-06	2.0039	5.4129e-06	2.0053
	1/320	1.7942e-06	2.0043	1.3481e-06	2.0054
0.99	1/20	4.4594e-04	–	3.3783e-04	–
	1/40	1.1142e-04	2.0009	8.4333e-05	2.0021
	1/80	2.7789e-05	2.0034	2.1014e-05	2.0047
	1/160	6.9273e-06	2.0042	5.2338e-06	2.0054
	1/320	1.7265e-06	2.0045	1.3033e-06	2.0057

is given in Example 1. In MATLAB code, we take the commands of generating matrices as the start point of `Time1`, and in the rest of tables, “**Speed-up**” denotes  $\frac{\text{Time1}}{\text{Time}k}$  ( $k = 2, 3, 4$ ) and “**Iter**” is the average number of iterations required for solving the TSADE problem, namely,

$$\text{Iter} = \frac{1}{M} \sum_{m=1}^M \text{Iter}(m),$$

where  $\text{Iter}(m)$  represents the number of iterations required for solving (3.1). As for GPBiCOR( $m, \ell$ ) method [49] with circulant preconditioners in this example, a large number of experiments reveal that the results are better than others, when  $m = 3$  and  $\ell = 1$ . Some eigenvalue plots about both original and preconditioned matrices are drawn in Figs. 5-6. These two figures confirm that for circulant preconditioning, the eigenvalues of preconditioned matrices are clustered at 1 except for a few of them. That is to say, the vast majority of the eigenvalues are well separated away from 0. We validate the effectiveness and robustness of the designed circulant preconditioner from the respective of clustering spectrum distribution.

The numerical results in Example 3 are presented in Tables 9-10, reflecting that the average iterations of the three Krylov subspace methods with circulant preconditioners have little difference. In other words, the number of average iterations of these methods is about 7. On the other hand, the CPU time by the three Krylov subspace methods with circulant preconditioners are much less than that by LU factorization method as  $M$  and  $N$  become large. When  $M = N = 2^{11}$  in Table 9, the CPU time is about 95 seconds, and the **Speed-up** is almost 4.5, especially for

PBiCGSTAB method, the **Speed-up** can reach about 5. At the same case, in Table 10 the CPU time is about 110 seconds, and the **Speed-up** is almost 4. Meanwhile, although **Time1** required by LU factorization method for small text problems ( $M = N = 2^7, 2^8$ ) is the cheapest among other three methods (i.e. PBiCGSTAB, PBiCRSTAB and PGPBiCOR( $m, \ell$ )), our proposed methods are still more attractive in aspects of the lower memory requirement.

Table 9: CPU time in seconds for solving Example 1 with  $\theta = 0.7$ ,  $\alpha = 0.6$ ,  $\beta = 1.99$ ,  $d_+ = 0.7$ ,  $d_- = 0.9$ ,  $e_+ = 0.2$  and  $e_- = 0.6$ .

$h = \tau$	PBiCGSTAB			PBiCRSTAB		PGPBiCOR(3,1)	
	Time1	Time2(Iter)	Speed-up	Time3(Iter)	Speed-up	Time4(Iter)	Speed-up
$2^{-7}$	0.117	0.311(6.0)	0.37	0.338(6.0)	0.34	0.304(5.0)	0.38
$2^{-8}$	0.785	0.801(6.0)	0.98	0.857(6.0)	0.92	0.867(5.7)	0.91
$2^{-9}$	7.073	3.614(6.0)	1.96	3.802(6.0)	1.86	3.979(6.0)	1.78
$2^{-10}$	55.952	14.720(6.9)	3.80	14.209(6.0)	3.94	14.669(6.0)	3.81
$2^{-11}$	445.959	90.092(6.0)	4.95	95.151(6.0)	4.69	97.450(6.0)	4.58

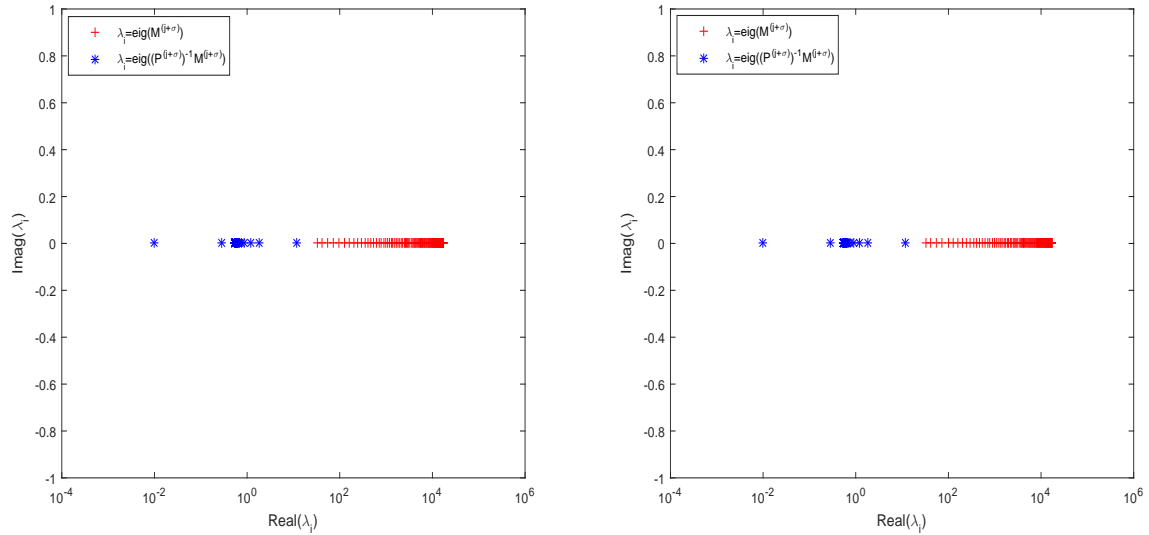


Fig. 5: Spectrum of both original and preconditioned matrices, when  $M = N = 2^7$ ,  $\theta = 0.7$ ,  $\alpha = 0.6$ ,  $\beta = 1.99$ ,  $d_+ = 0.7$ ,  $d_- = 0.9$ ,  $e_+ = 0.2$  and  $e_- = 0.6$ . Left: Time level  $j = 0$ ; Right: Time level  $j = 1$ .

Table 10: CPU time in seconds for solving Example 1 with  $\theta = 0.5$ ,  $\alpha = 0.8$ ,  $\beta = 1.9$ ,  $d_+ = 0.7$ ,  $d_- = 0.9$ ,  $e_+ = 0.2$  and  $e_- = 0.6$ .

$h = \tau$	PBiCGSTAB			PBiCRSTAB		PGPBiCOR(3,1)	
	Time1	Time2(Iter)	Speed-up	Time3(Iter)	Speed-up	Time4(Iter)	Speed-up
$2^{-7}$	0.130	0.355(7.0)	0.37	0.381(7.0)	0.34	0.341(6.0)	0.38
$2^{-8}$	0.851	0.889(7.0)	0.96	0.955(7.0)	0.89	0.896(6.0)	0.95
$2^{-9}$	7.267	3.966(7.0)	1.83	4.220(7.0)	1.72	3.989(6.0)	1.82
$2^{-10}$	57.173	15.469(7.7)	3.70	15.561(7.0)	3.67	14.730(6.0)	3.88
$2^{-11}$	461.713	113.397(8.7)	4.07	111.850(7.0)	4.13	105.410(6.9)	4.38

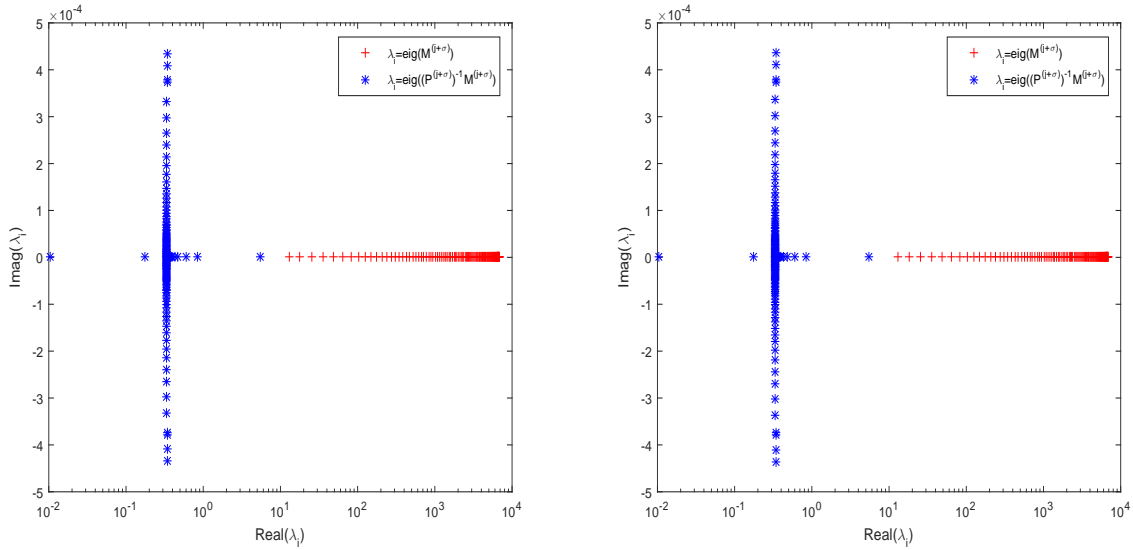


Fig. 6: Spectrum of both original and preconditioned matrices, when  $M = N = 2^7$ ,  $\theta = 0.5$ ,  $\alpha = 0.8$ ,  $\beta = 1.9$ ,  $d_+ = 0.7$ ,  $d_- = 0.9$ ,  $e_+ = 0.2$  and  $e_- = 0.6$ . Left: Time level  $j = 0$ ; Right: Time level  $j = 1$ .

**Example 4.** In this example, the exact solution and source term are given in Example 2, and we denote that  $d_{\pm,i}^{j+\sigma} = d_{\pm}(x_i, t_{j+\sigma})$  and  $e_{\pm,i}^{j+\sigma} = e_{\pm}(x_i, t_{j+\sigma})$ . Furthermore, the circulant preconditioner, in this example, is defined as

$$P^{(j+\sigma)} = \begin{cases} \frac{\tau^{-\theta}}{\Gamma(2-\theta)} a_0^{(\theta,\sigma)} I + \sigma \left( \frac{\bar{d}_+^{j+\sigma}}{h^\alpha} s(A_\alpha) + \frac{\bar{d}_-^{j+\sigma}}{h^\alpha} s(A_\alpha^T) \right. \\ \quad \left. - \frac{\bar{e}_+^{j+\sigma}}{h^\beta} s(A_\beta) - \frac{\bar{e}_-^{j+\sigma}}{h^\beta} s(A_\beta^T) \right), & j = 0, \\ \frac{\tau^{-\theta}}{\Gamma(2-\theta)} (a_0^{(\theta,\sigma)} + b_1^{(\theta,\sigma)}) I + \sigma \left( \frac{\bar{d}_+^{j+\sigma}}{h^\alpha} s(A_\alpha) + \frac{\bar{d}_-^{j+\sigma}}{h^\alpha} s(A_\alpha^T) \right. \\ \quad \left. - \frac{\bar{e}_+^{j+\sigma}}{h^\beta} s(A_\beta) - \frac{\bar{e}_-^{j+\sigma}}{h^\beta} s(A_\beta^T) \right), & j = 1, \dots, M-1, \end{cases}$$

where  $\bar{d}_{\pm}^{j+\sigma} = \frac{1}{N-1} \sum_{i=1}^{N-1} d_{\pm,i}^{j+\sigma}$  and  $\bar{e}_{\pm}^{j+\sigma} = \frac{1}{N-1} \sum_{i=1}^{N-1} e_{\pm,i}^{j+\sigma}$ . As for GPBiCOR( $m, \ell$ ) method [49] with circulant preconditioners in this example, a large number of experiments reveal that the results are better than others, when  $m = 3$  and  $\ell = 1$ . Some eigenvalue plots about both original and preconditioned matrices are drawn in Figs. 7-8. These two figures confirm that for circulant preconditioning, the eigenvalues of preconditioned matrices are clustered at 1 except for a few of them. That is to say, the vast majority of the eigenvalues are well separated away from 0. We validate the effectiveness and robustness of the designed circulant preconditioner from the respective of clustering spectrum distribution.

The numerical results in Example 4 are displayed in Tables 11-12, implying that the average iterations of the three Krylov subspace methods with circulant preconditioners are little different. In other words, the number of average iterations of these methods is about 12. On the other hand, the CPU time by the three Krylov subspace methods with circulant preconditioners are much less than that by LU factorization method as  $M$  and  $N$  become large. When  $M = N = 2^{10}$  in Table 11, the CPU time is about 29 seconds, and the **Speed-up** is almost 27, especially for PBiCRSTAB method, the **Speed-up** can reach about 32. At the same case, Table 12 indicates that the CPU time is about 30 seconds, and the **Speed-up** is almost 40, except for PGPBiCOR(3,1). Meanwhile, although **Time1** required by LU factorization method for small text problems ( $M = N = 2^6, 2^7$ ) is the cheapest among other three methods (i.e. PBiCGSTAB, PBiCRSTAB and PGPBiCOR( $m, \ell$ )), our proposed methods are still more attractive in aspects of the lower memory requirement. As a conclusion, our proposed IDS with fast solution techniques is still more practical than LU factorization method.

Table 11: CPU time in seconds for solving Example 2 with  $\theta = 0.9, \alpha = 0.8, \beta = 1.9$ .

$h = \tau$	PBiCGSTAB			PBiCRSTAB		PGPBiCOR(3, 1)	
	Time1	Time2(Iter)	Speed-up	Time3(Iter)	Speed-up	Time4(Iter)	Speed-up
$2^{-6}$	0.061	0.268(12.172)	0.23	0.323(12.672)	0.19	0.279(11.656)	0.22
$2^{-7}$	0.410	0.839(12.117)	0.49	0.959(12.727)	0.43	0.849(11.914)	0.48
$2^{-8}$	5.654	2.222(12.492)	2.54	2.218(12.438)	2.55	2.317(11.922)	2.44
$2^{-9}$	66.982	8.639(12.727)	7.75	8.248(12.248)	8.12	9.030(11.930)	7.42
$2^{-10}$	828.878	29.832(13.186)	27.78	25.840(11.957)	32.08	30.692(11.966)	27.01

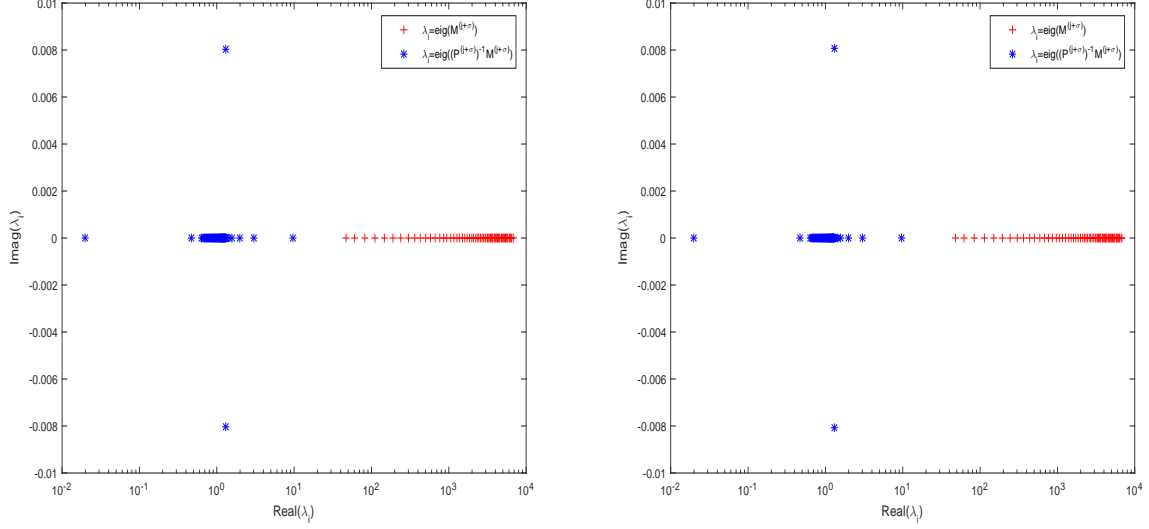


Fig. 7: Spectrum of both original and preconditioned matrices, when  $M = N = 2^6$ ,  $\theta = 0.9$ ,  $\alpha = 0.8$ ,  $\beta = 1.9$ . Left: Time level  $j = 0$ ; Right: Time level  $j = 1$ .

Table 12: CPU time in seconds for solving Example 2 with  $\theta = 0.7$ ,  $\alpha = 0.6$ ,  $\beta = 1.5$ .

$h = \tau$	PBiCGSTAB			PBiCRSTAB		PGPBiCOR(3,1)	
	Time1	Time2(Iter)	Speed-up	Time3(Iter)	Speed-up	Time4(Iter)	Speed-up
$2^{-6}$	0.061	0.242(11.359)	0.25	0.316(11.406)	0.19	0.291(11.594)	0.21
$2^{-7}$	0.407	0.794(12.211)	0.51	0.942(12.070)	0.43	0.882(11.820)	0.46
$2^{-8}$	5.939	1.981(12.945)	3.00	2.314(13.055)	2.57	2.465(12.297)	2.41
$2^{-9}$	74.497	7.977(13.289)	9.34	8.809(13.219)	8.46	9.714(12.775)	7.67
$2^{-10}$	1133.348	26.374(13.633)	42.97	28.174(13.307)	40.23	32.461(12.957)	34.91

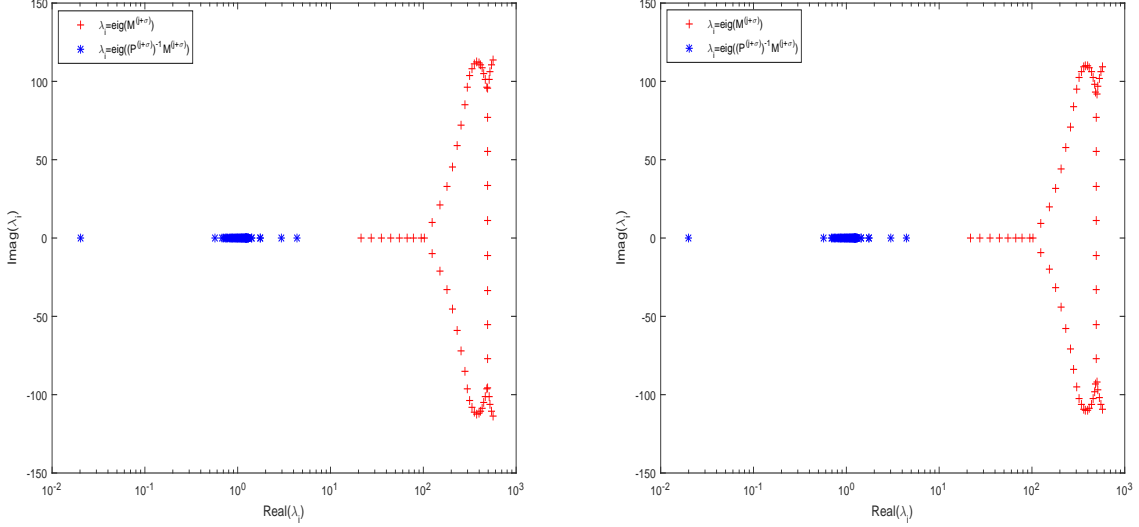


Fig. 8: Spectrum of both original and preconditioned matrices, when  $M = N = 2^7$ ,  $\theta = 0.7$ ,  $\alpha = 0.6$ ,  $\beta = 1.5$ . Left: Time level  $j = 0$ ; Right: Time level  $j = 1$ .

## 5 Conclusion

We now see, the new difference schemes of the second approximation order in space and the second order in time for the TSADE with variable coefficients are constructed as well. Furthermore, we find that when the diffusion coefficients satisfy some conditions, which are related to  $x$  and  $t$ , the convergence order of the IDM (2.4) is still  $\mathcal{O}(\tau^2 + h^2)$ . Then, a plenty of numerical tests have shown that our implicit difference scheme converges with second-order accuracy in both time and space. More significantly, with the help of (3.1), we can ameliorate the calculation skill by the implementation of reliable preconditioning iterative techniques, with only computational cost and memory of  $\mathcal{O}(N \log N)$  and  $\mathcal{O}(N)$ , respectively. Numerical experiments strongly support that the efficiency of the proposed preconditioning methods.

## Acknowledgments

*This work is supported by the 973 Program (2013CB329404), National Science Foundation of China (NSFC) (61370147), the Scientific Research Fund of SiChuan Provincial Education Department (15ZA0288).*

## Appendix

---

**Algorithm 1** GPBiCOR(3,1) for  $Ax = b$  with preconditioner  $K$ .

---

1: Select initial guess $\mathbf{x}_0$ and $\mathbf{r}_0 = \mathbf{b} - A\mathbf{x}_0$ 2: Choose $\mathbf{r}_0^* = AK^{-1}\mathbf{r}_0$ s.t. $(\mathbf{r}_0^*, AK^{-1}\mathbf{r}_0) \neq 0$ . Set $\mathbf{t}_{-1} = \mathbf{w}_{-1} = \mathbf{u}_{-1} = \hat{\mathbf{u}}_{-1} = \mathbf{0}$ , $\beta_{-1} = 0$ , $\mathbf{e}_0 = K^{-1}\mathbf{r}_0$ , $\hat{\mathbf{e}}_0 = A\mathbf{e}_0$ . 3: <b>for</b> $n = 0, 1, \dots$ , until convergence <b>do</b> 4: $\mathbf{p}_n = \mathbf{e}_n + \beta_{n-1}(\mathbf{p}_{n-1} - \mathbf{u}_{n-1})$ 5: $\hat{\mathbf{p}}_n = \hat{\mathbf{e}}_n + \beta_{n-1}(\hat{\mathbf{p}}_{n-1} - \hat{\mathbf{u}}_{n-1})$ 6:   Solve $K\mathbf{h}_n = \hat{\mathbf{p}}_n$ 7:   Compute $\mathbf{g}_n = A\mathbf{h}_n$ and then $\alpha_n = \frac{(\mathbf{r}_0^*, \mathbf{e}_n)}{(\mathbf{r}_0^*, \mathbf{g}_n)}$ 8: $\mathbf{t}_n = \mathbf{r}_n - \alpha_n \hat{\mathbf{p}}_n$ 9: $\mathbf{y}_n = \mathbf{t}_{n-1} - \mathbf{t}_n - \alpha_n \mathbf{q}_{n-1}$ 10: $\mathbf{s}_n = \mathbf{e}_n - \alpha_n \mathbf{h}_n$ ( $\triangleright \mathbf{s}_n \triangleq K^{-1}\mathbf{t}_n$ ) 11: $\mathbf{w}_n = \hat{\mathbf{e}}_n - \alpha_n \mathbf{g}_n$ ( $\triangleright \mathbf{w}_n \triangleq A\mathbf{s}_n$ ) 12: <b>if</b> $(\text{mod}(n, 4) < 3$ or $n = 0)$ <b>then</b> 13: $\xi = \frac{(\mathbf{w}_n, \mathbf{t}_n)}{(\mathbf{w}_n, \mathbf{w}_n)}$ (Hint: $\eta_n = 0$ ) 14: $\mathbf{u}_n = \xi_n \mathbf{h}_n$ , $\hat{\mathbf{u}}_n = \xi_n \mathbf{g}_n$	15: $\mathbf{z}_n = \xi_n \mathbf{e}_n - \alpha_n \mathbf{u}_n$ 16: $\mathbf{r}_{n+1} = \mathbf{t}_n - \xi_n \mathbf{w}_n$ 17: <b>else</b> 18: $\xi_n = \frac{(\mathbf{y}_n, \mathbf{y}_n)(\mathbf{w}_n, \mathbf{t}_n) - (\mathbf{y}_n, \mathbf{t}_n)(\mathbf{w}_n, \mathbf{y}_n)}{(\mathbf{w}_n, \mathbf{w}_n)(\mathbf{y}_n, \mathbf{y}_n) - (\mathbf{y}_n, \mathbf{w}_n)(\mathbf{w}_n, \mathbf{y}_n)}$ 19: $\eta_n = \frac{(\mathbf{w}_n, \mathbf{w}_n)(\mathbf{y}_n, \mathbf{t}_n) - (\mathbf{y}_n, \mathbf{w}_n)(\mathbf{w}_n, \mathbf{t}_n)}{(\mathbf{w}_n, \mathbf{w}_n)(\mathbf{y}_n, \mathbf{y}_n) - (\mathbf{y}_n, \mathbf{w}_n)(\mathbf{w}_n, \mathbf{y}_n)}$ 20: $\mathbf{u}_n = \xi_n \mathbf{h}_n + \eta_n(\mathbf{s}_{n-1} - \mathbf{e}_n + \beta_{n-1} \mathbf{u}_{n-1})$ 21: $\hat{\mathbf{u}}_n = \xi_n \mathbf{g}_n + \eta_n(\mathbf{w}_{n-1} - \hat{\mathbf{e}}_n + \beta_{n-1} \hat{\mathbf{u}}_{n-1})$ 22: $\mathbf{z}_n = \xi_n \mathbf{e}_n + \eta_n \mathbf{z}_{n-1} - \alpha_n \mathbf{u}_n$ 23: $\mathbf{r}_{n+1} = \mathbf{t}_n - \eta_n \mathbf{y}_n - \xi_n \mathbf{w}_n$ 24: <b>endif</b> 25:   Solve $K\mathbf{e}_{n+1} = \mathbf{r}_{n+1}$ 26:   Compute $\hat{\mathbf{e}}_{n+1} = A\mathbf{e}_{n+1}$ 27: $\beta_n = \frac{\alpha_n}{\xi_n} \cdot \frac{(\mathbf{r}_0^*, \hat{\mathbf{e}}_{n+1})}{(\mathbf{r}_0^*, \hat{\mathbf{e}}_n)}$ 28: $\mathbf{x}_{n+1} = \mathbf{x}_n + \alpha_n \mathbf{p}_n + \mathbf{z}_n$ 29: $\mathbf{q}_n = \mathbf{w}_n + \beta_n \hat{\mathbf{p}}_n$ 30: <b>end for</b>
---	--

---

## References

- [1] F. Liu, P. Zhuang, V. Anh, I. Turner, K. Burrage, Stability and convergence of the difference methods for the space-time fractional advection-diffusion equation, *Appl. Math. Comput.*, 191 (2007), pp. 12-20.
- [2] Z. Zhao, X.-Q. Jin, M.-M. Lin, Preconditioned iterative methods for space-time fractional advection-diffusion equations, *J. Comput. Phys.*, 319 (2016), pp. 266-279.
- [3] I. Podlubny, Fractional Differential Equations, vol. 198 of Mathematics in Science and Engineering, Academic Press, Inc., San Diego, CA, 1999.
- [4] S. G. Samko, A. A. Kilbas, O. I. Marichev, Fractional Integrals and Derivatives: Theory and Applications, Gordon and Breach Science Publishers, Yverdonn, 1993.
- [5] D. A. Benson, R. Schumer, M. M. Meerschaert, S. W. Wheatcraft, Fractional dispersion, Lévy motion, and the MADE tracer tests, *Transport in Porous Media*, 42 (2001), pp. 211-40.
- [6] D. A. Benson, S. W. Wheatcraft, M. M. Meerschaert, The fractional-order governing equation of Lévy motion, *Water Resour. Res.*, 36 (2000), pp. 1413-23.
- [7] R. Metzler, J. Klafter, The random walks guide to anomalous diffusion: a fractional dynamics approach, *Phys. Rep.*, 339 (2000), pp. 1-77.
- [8] Y. Povstenko, Generalized boundary conditions for the time-fractional advection diffusion equation, *Entropy*, 17 (2015), pp. 4028-4039.
- [9] D. A. Benson, S. W. Wheatcraft, M. M. Meerschaert, Application of a fractional advection-dispersion equation, *Water Resour. Res.*, 36 (2000), pp. 1403-1412.
- [10] S. Momani, An algorithm for solving the fractional convection-diffusion equation with nonlinear source term, *Commun. Nonlinear Sci. Numer. Simul.*, 12 (2007), pp. 1283-1290.
- [11] S. Gupta, D. Kumar, J. Singh, Analytical solutions of convection-diffusion problems by combining Laplace transform method and homotopy perturbation method, *Alexandria Engineering Journal*, 54 (2015), pp. 645-651.

- [12] S. Abbasbandy, S. Kazem, M. S. Alhuthali, H. H. Alsulami, Application of the operational matrix of fractional-order Legendre functions for solving the time-fractional convection-diffusion equation, *Appl. Math. Comput.*, 266 (2015), pp. 31-40.
- [13] V. J. Ervin, N. Heuer, J. P. Roop, Numerical approximation of a time dependent, nonlinear, space-fractional diffusion equation, *SIAM J. Numer. Anal.*, 45 (2007), pp. 572-591.
- [14] N. J. Ford, A. C. Simpson, The numerical solution of fractional differential equations: speed versus accuracy, *Numer. Algorithms*, 26 (2001), pp. 333-346.
- [15] F. Liu, V. Anh, I. Turner, Numerical solution of the space fractional Fokker-Planck equation, *J. Comput. Appl. Math.*, 166 (2004), pp. 209-219.
- [16] M. M. Meerschaert, C. Tadjeran, Finite difference approximations for fractional advection-dispersion flow equations, *J. Comput. Appl. Math.*, 172 (2004), pp. 65-77.
- [17] M. M. Meerschaert, C. Tadjeran, Finite difference approximations for two-sided spacefractional partial differential equations, *Appl. Numer. Math.*, 56 (2006), pp. 80-90.
- [18] M. M. Meerschaert, H. P. Scheffler, C. Tadjeran, Finite difference methods for two-dimensional fractional dispersion equation, *J. Comput. Phys.*, 211 (2006), pp. 249-261.
- [19] H. Wang, K. Wang, T. Sircar, A direct  $\mathcal{O}(N \log 2N)$  finite difference method for fractional diffusion equations, *J. Comput. Phys.*, 229 (2010), pp. 8095-8104.
- [20] W.-H. Luo, T.-Z. Huang, G.-C. Wu, X.-M. Gu, Quadratic spline collocation method for the time fractional subdiffusion equation, *Applied Mathematics and Computation*, 276 (2016), pp. 252C265.
- [21] X.-M. Gu, T.-Z. Huang, X.-L. Zhao, H.-B. Li, L. Li, Strang-type preconditioners for solving fractional diffusion equations by boundary value methods, *Journal of Computational and Applied Mathematics*, 277 (2015), pp. 73-86.
- [22] L. Wei, X. Zhang, Y. He, Analysis of a local discontinuous Galerkin method for timefractional advection-diffusion equations, *International Journal of Numerical Methods for Heat & Fluid Flow*, 23 (2013), pp. 634 - 648.
- [23] P. Zhuang, Y.-T. Gu, F. Liu, I. Turner, P.K.D.V. Yarlagadda, Time-dependent fractional advection-diffusion equations by an implicit MLS meshless method, *Int. J. Numer. Meth. Eng.*, 88 (2011), pp. 1346-1362.
- [24] F. Liu, P. Zhuang, K. Burrage, Numerical methods and analysis for a class of fractional advection-dispersion models, *Comput. Math. Appl.*, 64 (2012), pp. 2990-3007.
- [25] E. Sousa, C. Li, A weighted finite difference method for the fractional diffusion equation based on the Riemann-Liouville derivative, *Appl. Num. Math.*, 90 (2015), pp. 22-37.
- [26] W. Qu, S.-L. Lei, S.-W. Vong, Circulant and skew-circulant splitting iteration for fractional advection-diffusion equations, *Int. J. Comput. Math.*, 91 (2014), pp. 2232-2242.
- [27] Z. Wang, S. Vong, A high-order exponential ADI scheme for two dimensional time fractional convection-diffusion equations, *Comput. Math. Appl.*, 68 (2014), pp. 185-196.
- [28] Z.-J. Fu, W. Chen, H.-T. Yang, Boundary particle method for Laplace transformed time fractional diffusion equations, *J. Comput. Phys.*, 235 (2013), pp. 52-66.
- [29] S. Zhai, X. Feng, Y. He, An unconditionally stable compact ADI method for three-dimensional time-fractional convection-diffusion equation, *J. Comput. Phys.*, 269 (2014), pp. 138-155.
- [30] Y.-M. Wang, A compact finite difference method for solving a class of time fractional convection-subdiffusion equations, *BIT*, 55 (2015), pp. 1187-1217.

- [31] Y. Zhang, A finite difference method for fractional partial differential equation, *Appl. Math. Comput.*, 215 (2009), pp. 524-529.
- [32] Y. Zhang, Finite difference approximations for space-time fractional partial differential equation, *J. Numer. Math.*, 17 (2009), pp. 319-326.
- [33] Y. Shao, W. Ma, Finite difference approximations for the two-side space-time fractional advection-diffusion equations, *J. Comput. Anal. Appl.*, 21 (2016), pp. 369-379.
- [34] P. Qin, X. Zhang, A numerical method for the space-time fractional convection-diffusion equation, *Math. Numer. Sin.*, 30 (2008), pp. 305-310. (in Chinese)
- [35] S. Shen, F. Liu, V. Anh, Numerical approximations and solution techniques for the space-time Riesz-Caputo fractional advection-diffusion equation, *Numer. Algorithms*, 56 (2011), pp. 383-403.
- [36] J. Wei, Y. Chen, B. Li, M. Yi, Numerical solution of space-time fractional convection-diffusion equations with variable coefficients using Haar wavelets, *Comput. Model. Eng. Sci. (CMES)*, 89 (2012), pp. 481-495.
- [37] H. Hejazi, T. Moroney, F. Liu, A finite volume method for solving the two-sided time-space fractional advection-dispersion equation, *Cent. Eur. J. Phys.*, 11 (2013), pp. 1275-1283.
- [38] S. Irandoust-pakchin, M. Dehghan, S. Abdi-mazraeh, M. Lakestani, Numerical solution for a class of fractional convection-diffusion equations using the flatlet oblique multiwavelets, *J. Vib. Control*, 20 (2014), pp. 913-924.
- [39] M. Parvizi, M. R. Eslahchi, M. Dehghan, Numerical solution of fractional advection-diffusion equation with a nonlinear source term, *Numer. Algor.*, 68 (2015), pp. 601-629.
- [40] N. J. Ford, K. Pal, Y. Yan, An algorithm for the numerical solution of two-sided space fractional partial differential equations, *Comput. Methods Appl. Math.*, 15 (2015), pp. 497-514.
- [41] M. Cui, Compact exponential scheme for the time fractional convection-diffusion reaction equation with variable coefficients, *J. Comput. Phys.*, 280 (2015), pp. 143-163.
- [42] H. Wang, K. Wang, T. Sircar, A direct  $\mathcal{O}(N \log^2 N)$  finite difference method for fractional diffusion equations, *J. Comput. Phys.*, 229 (2010), pp. 8095-8104.
- [43] M. Ng, *Iterative Methods for Toeplitz Systems*, Oxford University Press, New York, 2004.
- [44] K. Wang, H. Wang, A fast characteristic finite difference method for fractional advection-diffusion equations, *Adv. Water Resour.*, 34 (2011), pp. 810-816.
- [45] X.-M. Gu, T.-Z. Huang, H.-B. Li, L. Li, W.-H. Luo, On  $k$ -step CSCS-based polynomial preconditioners for Toeplitz linear systems with application to fractional diffusion equations, *Applied Mathematics Letters*, 42 (2015), pp. 53-58.
- [46] Y.-Q. Bai, T.-Z. Huang, X.-M. Gu, Circulant preconditioned iterations for fractional diffusion equations based on Hermitian and skew-Hermitian splittings, *Applied Mathematics Letters*, 48 (2015), pp. 14-22.
- [47] S.-F. Wang, T.-Z. Huang, X.-M. Gu, W.-H. Luo, Fast permutation preconditioning for fractional diffusion equations, *SpringerPlus*, 5 (2016):1109, DOI 10.1186/s40064-016-2766-4.
- [48] H. A. van der Vorst, Bi-CGSTAB: A fast and smoothly converging variant of Bi-CG for the solution of nonsymmetric linear systems, *SIAM J. Sci. Stat. Comput.*, 13 (1992), pp. 631-644.
- [49] X.-M. Gu, T.-Z. Huang, B. Carpentieri, L. Li, C. Wen, A hybridized iterative algorithm of the BiCORSTAB and GPBiCOR methods for solving non-Hermitian linear systems, *Comput. Math. Appl.*, 70 (2015), pp. 3019-3031.

- [50] A. A. Alikhanov, A new difference scheme for the time fractional diffusion equation, *J. Comput. Phys.*, 280 (2015), pp. 424-438.
- [51] W.-Y. Tian, H. Zhou, W.-H. Deng, A class of second order difference approximations for solving space fractional diffusion equations, *Math. Comput.*, 84 (2015), pp. 1703-1727.
- [52] L.-B. Feng, P. Zhuang, F. Liu, I. Turner, J. Li, High-order numerical methods for the Riesz space fractional advection-dispersion equations, *Comput. Math. Appl.*, (2016). Available online at <http://dx.doi.org/10.1016/j.camwa.2016.01.015>.
- [53] A. Mohebbi, M. Abbaszadeh, M. Dehghan, A high-order and unconditionally stable scheme for the modified anomalous fractional sub-diffusion equation with a nonlinear source term, *J. Comput. Phys.*, 240 (2013), pp. 36-48.
- [54] M. Dehghan, M. Safarpour, M. Abbaszadeh, Two high-order numerical algorithms for solving the multi-term time fractional diffusion-wave equations, *J. Comput. Appl. Math.*, 290 (2015), pp. 174-195.
- [55] S.-L. Lei, H.-W. Sun, A circulant preconditioner for fractional diffusion equations, *J. Comput. Phys.*, 242 (2013), pp. 715-725.
- [56] R. Chan, X. Jin, *An Introduction to Iterative Toeplitz Solvers*, SIAM, Philadelphia, 2007.
- [57] R. Varga, *Geršgorin and His Circles*, Berlin: Springer-Verlag, 2004.
- [58] X.-M. Gu, T.-Z. Huang, C.-C. Ji, B. Carpentierri, A. A. Alikhanov, Fast iterative method with a second-order implicit difference scheme for time-space fractional convection-diffusion equation, arXiv:1603.00279, 2016, 29 pages. Available online at <https://arxiv.org/abs/1603.00279>.